A LARGE-SIGNAL ANALYSIS OF BEAM-TYPE CROSSED-FIELD TRAVELING-WAVE TUBES

Thesis by
James W. Sedin

In Partial Fulfillment of the Requirements
For the Degree of
Doctor of Philosophy

California Institute of Technology
Pasadena, California

1958

ACKNOWLEDGMENT

I would like to express my thanks to Professors Roy W. Gould and Lester M. Field for their encouragement and assistance in this investigation.

Financial support has been extended by the Hughes Aircraft Company, the Westinghouse Electric Company, the Sperry Gyroscope Company, and the Office of Naval Research. Some of the preliminary calculations were carried out on ERA 1103 equipment that was provided through the courtesy of the Electrical Engineering Department of the University of Minnesota.

The numerical computations were made with the aid of Mr. Ken Ferrin.

ABSTRACT

The equations governing the behavior of beam-type, crossed-field, traveling-wave tubes are formulated and presented. The geometry is assumed to be two-dimensional. The electron beam is treated as a number of cylinders of charge (it can be regarded as a number of layers of pencils the axes of which are parallel; these pencils can move in the two dimensions perpendicular to their axes) and space-charge forces are included by calculating the field due to these cylinders when they are placed between two perfectly conducting planes. The nonlinear equations are re-expressed in terms of normalized variables suitable for machine computation, and the procedure for solving these equations numerically is discussed. The equations are solved for a number of thin-beam, small-signal cases and the results are compared with previous analytical work. Numerical difficulties are encountered because the electric field approaches infinity in the neighborhood of a line charge. These difficulties are circumvented by a modification of the electric field in the vicinity of a line charge. Large-signal calculations are carried out for the special case of a thin sheet beam which would travel in a straight line in the absence of r-f effects. The computations are carried out for both forward- and backward-wave interaction by using several values of a space-charge parameter that cover typical operating conditions.

TABLE OF CONTENTS

I. INTRODUCTION

The development[1] in recent years of successful amplifiers and voltage tunable oscillators for microwave frequencies that employ a stream of electrons traveling at right angles to mutually perpendicular static electric and magnetic fields has resulted in a renewed interest in the analysis of this type of device. These tubes exhibit the same high efficiency common to well-designed magnetrons and suffer from the same lack of quantitative understanding of their operation also common to magnetrons. The difficulty lies in the complicated nature of the electron trajectories and the seemingly inherent nonlinear nature of the interaction between the electrons and the propagating electromagnetic wave. The purpose of the work presented here is to obtain a set of equations which describe a physical model that retains the basic characteristics of these devices and to solve these equations for some particular cases of interest and investigate the effects of various parameters on the operating characteristics of crossed-field devices. The solutions actually carried out are mainly for backward-wave interaction at large-signal levels with various values of a defined space-charge parameter that cover typical operating situations. A few forward-wave cases are also computed and the results compared with the backward-wave cases. The equations obtained here are of sufficient scope that one might hope for quantitative agreement with experimental results in certain cases.

Crossed-field traveling-wave tubes can be grouped into two major categories:

1. Devices in which the beam is formed by an electron gun system and injected into the interaction region between a slow-wave circuit and a flat plate parallel to the circuit called the sole (Fig. 1a). This type of device will be referred to as a beam-type, crossed-field, traveling-wave tube.

2. Devices in which the electrode parallel to the circuit is an emitting surface and forms the cathode (Fig. 1b). This type of device will be referred to as a magnetron-type, crossed-field, traveling-wave tube.

Although this work was instigated by some experimental results related to a re-entrant beam amplifier device which falls into the second category, this analysis will be concerned with devices which lie exclusively in Group 1. The restriction to this group has been made because the beam is more clearly defined in such a device, and it is not necessary to make any basic assumptions about the nature of the beam that might predetermine to some degree the results that may be obtained. It is felt that the results obtained are qualitatively useful in discussing devices which fall into Group 2. The problem to be treated can be stated in very general terms. An electron beam focused by crossed static electric and magnetic fields is injected into a region in which an electromagnetic wave is propagating parallel to the direction of electron flow; determine the effects of the interaction between the wave and the beam. A brief qualitative description of this interaction in the absence of space-charge fields will serve both as a review and as an introduction to the problems encountered in the analysis of such

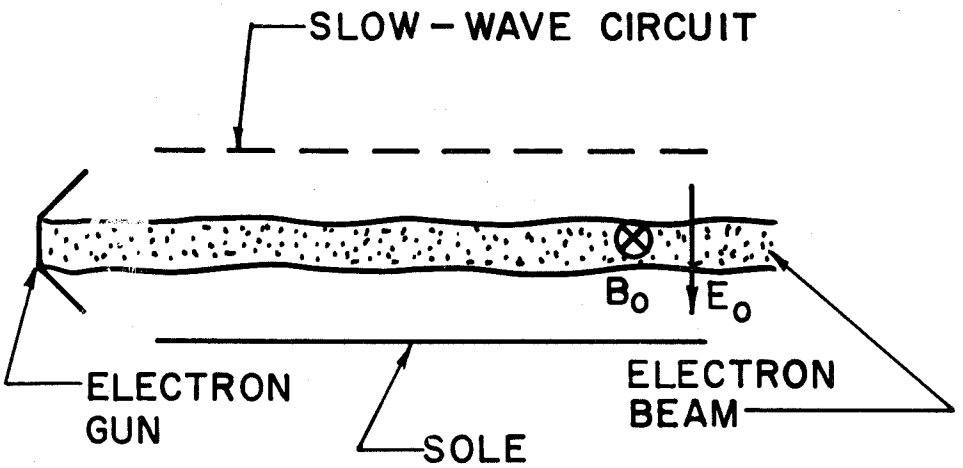

Fig. 1a. Schematic diagram of a beam-type, crossed-field traveling-wave tube

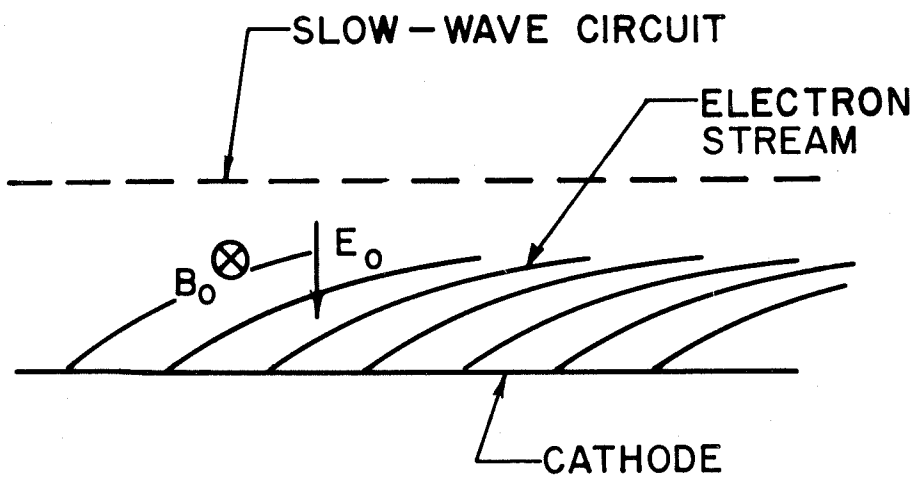

Fig. 1b. Schematic diagram of a magnetron-type, crossed-field, traveling-wave tube

a system. Electron motion in static electric and magnetic fields will be discussed first. The fields associated with the waves on a typical slow-wave circuit will then be introduced, and the wave-beam interaction described.

If an electron is injected into a region in which there is a static electric field $-E_o \hat{e}_y$ and a static magnetic field $+B_o \hat{e}_x$ (Fig. 2) with a velocity $\bar{u}$ which lies entirely in the yz plane, the trajectory of this electron will be some form of cycloid also in the yz plane. If $\bar{u}$ is $\bar{u}_o \hat{e}_z$, where $u_o = E_o/B_o$, the electron trajectory will be a straight line described by $y = y_o$ and $z = z_o + u_o t$, where y_o, z_o is the position of the electron at time $t = 0$. If the injection velocity is anything other than $u_o \hat{e}_z$, the average drift velocity in the z direction will still be $u_o = E_o/B_o$, but there will be an additional circular motion superimposed on this drift velocity. This result is easily seen by writing the equations of motion for the electron

$$m \frac{d^2y}{dt^2} = -eE_o - e \frac{dz}{dt} B_o; \quad m \frac{d^2z}{dt^2} = eB_o \frac{dy}{dt} \tag{I.1}$$

where m is the electronic mass and -e the electronic charge, and then making a nonrelativistic transformation to a coordinate system y, z' moving in the z direction with a velocity u_o (the entire treatment is nonrelativistic).

$$\frac{d^2y}{dt^2} = -\omega_c \frac{dz'}{dt}; \quad \frac{d^2z'}{dt^2} = \omega_c \frac{dy}{dt} \tag{I.2}$$

The electric field disappears and the problem reduces to finding

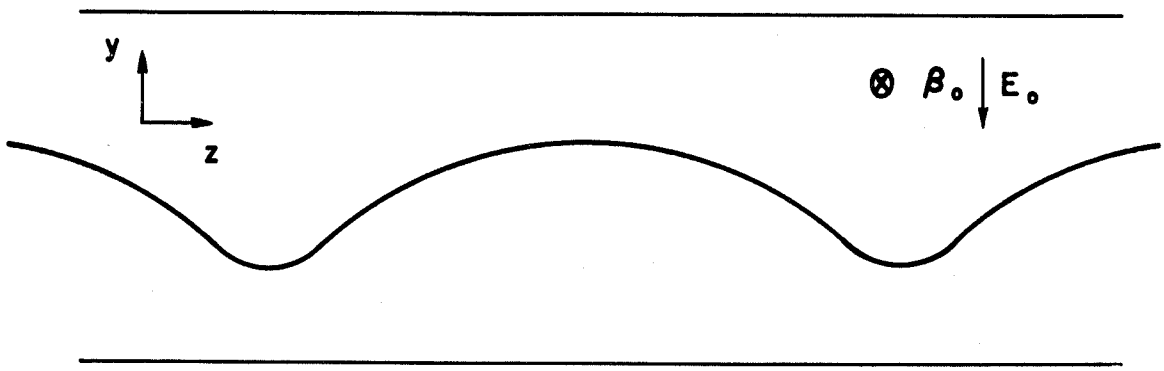

Fig. 2a. Hypocycloidal electron trajectory in crossed electric and magnetic fields

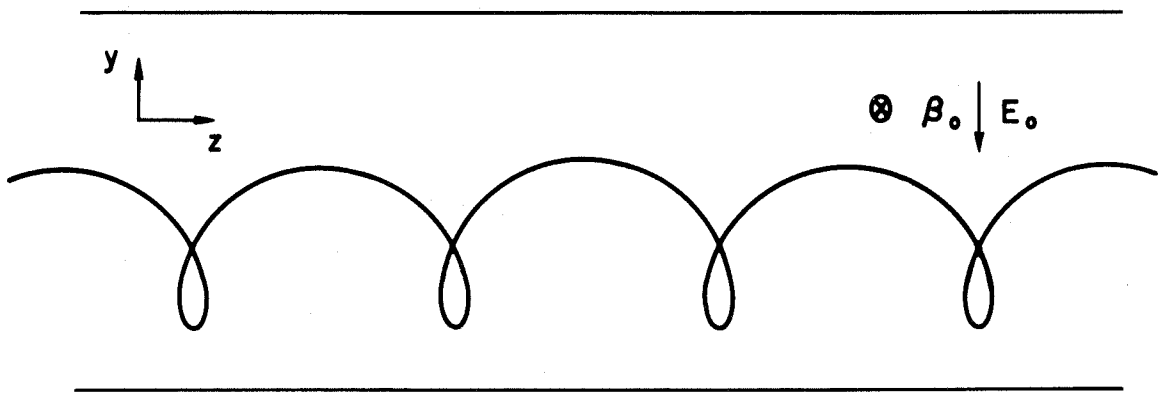

Fig. 2b. Epicycloidal electron trajectory in crossed electric and magnetic fields

the motion of an electron in a plane perpendicular to a magnetic field B_o. This motion is circular with an angular frequency $\omega_c = eB_o/m$ and a radius $r = v'/\omega_c$, where v' is the electron velocity in the moving coordinate system. The actual trajectories in the fixed system can be visualized by considering the motion of a point located at $r = v'/\omega_c$ on the radius of a wheel of radius $r = u_o/\omega_c$ as the wheel rolls. If v' is less than u_o, the trajectory will be a hypocycloid as illustrated in Fig. 2a, and if v' is greater than u_o, the trajectory will be an epicycloid as shown in Fig. 2b. An ideal injection system for a beam-type tube would have $v' = 0$, and the trajectories would be straight lines.

In order to obtain a net interaction effect, the circuit must propagate an electromagnetic wave at approximately the same velocity as the electron drift velocity $u_o = E_o/B_o$. This velocity is, of course, less than the velocity of light so that some complicated form of circuit must be used to reduce the phase velocity of the electromagnetic wave. A typical slow-wave circuit is shown in Fig. 3. The wave supported by such a structure can be expressed as an infinite sum of spatial harmonic components, and a frequency-propagation constant diagram for such a circuit including the harmonics would be similar to that shown in Fig. 4a. This diagram is for a forward-wave fundamental circuit because the phase and group velocities of the harmonic with the smallest phase shift have the same sign. Different forms of slow-wave circuits can be backward-wave fundamental and have ω-β diagrams similar to those in Fig. 4b. The electric fields associated with one of the spatial harmonics of one of these circuits are pictured in Fig. 5.

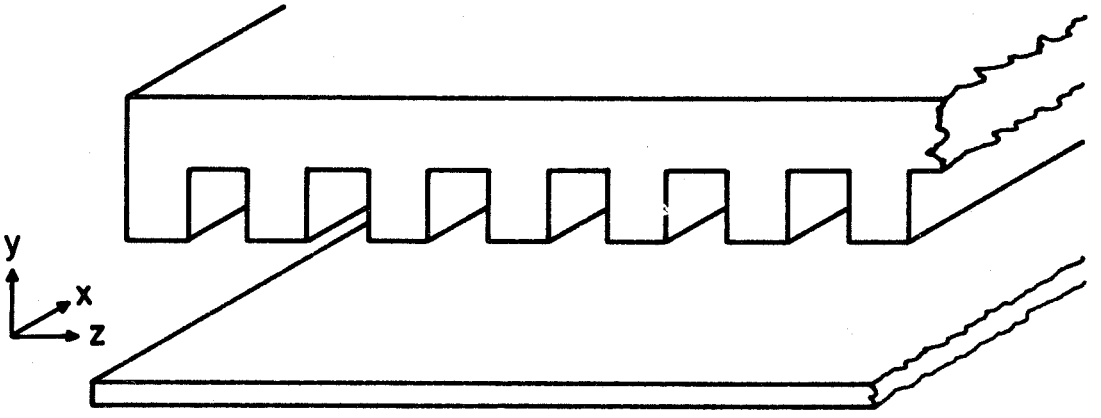

Fig. 3. A typical slow-wave circuit for crossed-field devices

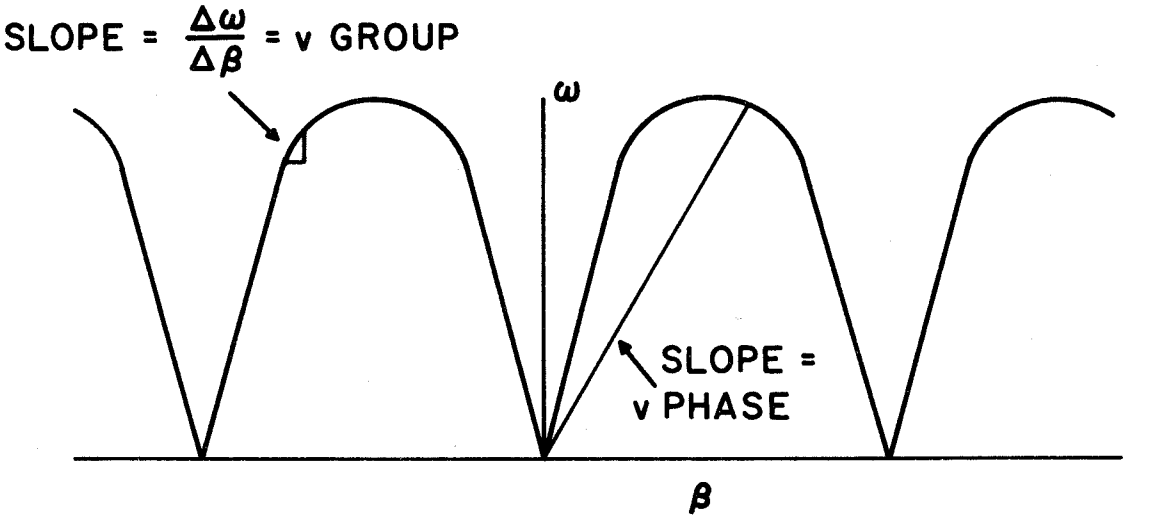

Fig. 4a. ω - β diagram for a fundamental forward-wave circuit

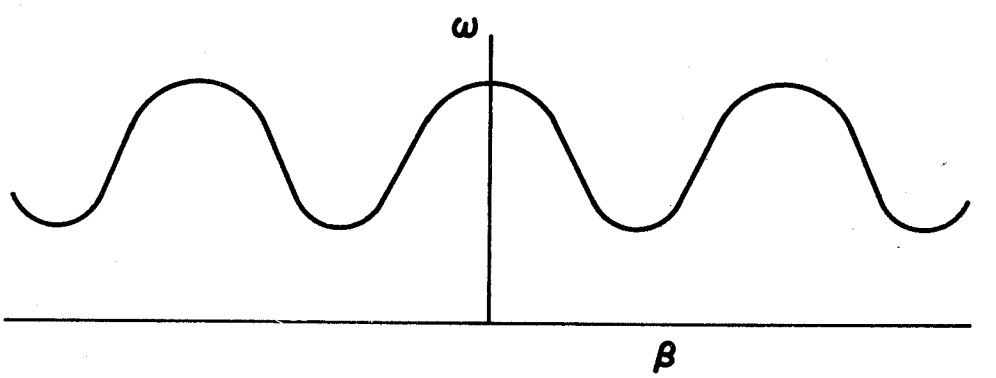

Fig. 4b. ω - β diagram for a fundamental backward-wave circuit

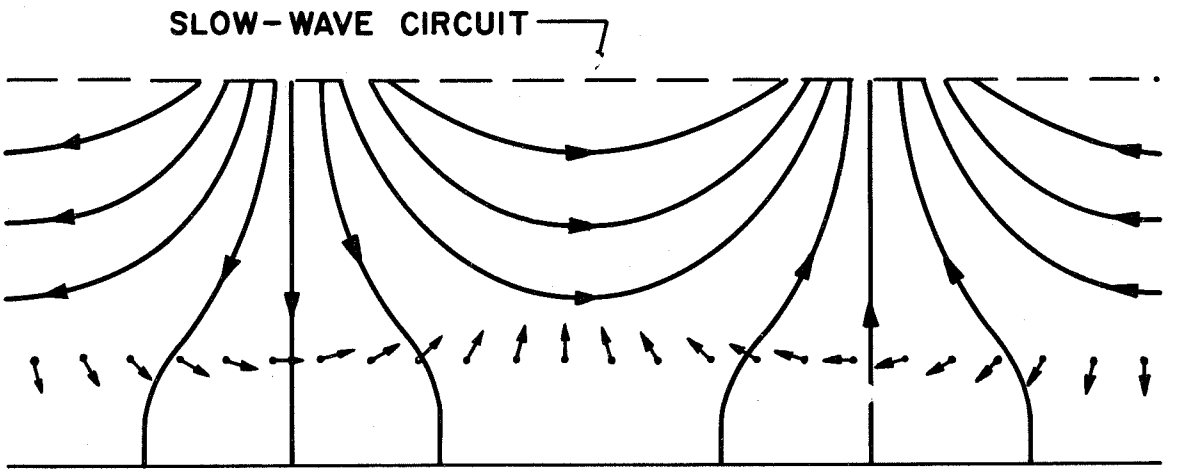

Fig. 5. Electric-field pattern of one spatial harmonic component of a slow-wave circuit

This entire pattern is moving in the z direction at the phase velocity of the wave. The magnetic fields associated with the wave are perpendicular to the plane of the paper, but they are not shown because the forces due to the alternating magnetic field are of the order of $(u_o/c)^2$ times the electric forces and will be neglected.

A very simple qualitative description of the interaction can be given for the case in which the average electron drift velocity is equal to the phase velocity of the wave. If one transforms to a coordinate system moving with this velocity, the field pattern is a static pattern as shown in Fig. 5, and the electrons in the beam are initially at rest in this pattern. The static electric field disappears, but the magnetic field B_o is still present, and if the magnetic field is large, the electrons move approximately at right angles to the applied electric field, as indicated by the small arrows on the dots representing the electron stream in Fig. 5. Rather than being slowed down or speeded up and exchanging kinetic energy for wave energy or vice versa, the electrons continue to move at essentially the same velocity, but they move into regions of different potential energy, and it is this difference in potential energy that appears as a difference in wave energy. It can be seen from Fig. 5 that the field pattern is such as to cause bunching in the region where the electrons are giving up potential energy so that more electrons are losing energy than are gaining it. The net effect is a decrease in potential energy of the beam, which results in wave amplification.

The quantitative analysis of the beam-type, crossed-field, traveling-wave tube has been treated by a number of workers under a variety of assumed conditions. Pierce[2] and Muller[3] have treated the case in which the space-charge forces are neglected, the beam is assumed to be a thin sheet in the transverse direction which travels in a straight line in the absence of r-f effects, and the amplitudes of all alternating quantities are small so that the equations can be linearized. This analysis was carried out by replacing the circuit with an equivalent transmission line and determining the current that drives this transmission line by converting the transverse motions of the electrons into an equivalent alternating charge density at the plane of the circuit.

Feinstein and Kino[4] have treated the same case but have not required that the equations be linearized. They do assume that the beam drift velocity and the wave velocity are in synchronism, and that the electric fields decay exponentially away from the circuit (this is equivalent to assuming that the sole is removed to infinity). Under these conditions, an integral equation is obtained for the circuit field which can be solved numerically.

Gould[5] has presented a field analysis of the linearized case which included space-charge forces, and allowed for a beam of finite thickness in laminar Brillouin flow. The differential equation for the electric field inside the beam is obtained, and for the special case where the electron drift velocity is approximately equal to the phase velocity of the circuit waves, the a-c charge density in the beam is zero, so that the equation for the field reduces to Laplace's equation ($u_o \ll c$). The field solution

is carried out by replacing the rippled boundary of the beam with an equivalent surface-charge density and matching the beam admittance to the admittance of the region outside of the beam across this equivalent plane boundary. The boundary condition at the circuit is matched by assuming that the admittance presented by the circuit to the interaction region is the same as the admittance with no beam present for all the space harmonics except the one nearly in synchronism with the beam. The admittance that this harmonic presents to the interaction region is expanded in a Taylor's series in the propagation constant about the value with no beam present, and the new propagation constant is determined by matching this admittance with the beam admittance. Gould [6] has also presented a simplified analysis of this type for a thin sheet beam, including space-charge effects.

The analysis presented here will eliminate as many as possible of the restrictive assumptions necessary in the above work and still leave a tractable set of equations. Specifically, the equations derived here will include space-charge forces, finite beam thickness, nonlaminar electron trajectories, nonsynchronism between circuit-wave velocity and average electron drift velocity, and nonlinear interaction effects. The techniques employed are similar to those used by Nordsieck,[7] Poulter, [8] Tien, [9] and Rowe [10] in the large-signal analysis of the ordinary traveling-wave tube. The beam is regarded as a finite number of charged particles, and the motion of each of these particles under the influence of the circuit fields and of all the other particles is computed. The effect of the beam on the circuit wave is determined by summing

the effects of all the individual particles. The equations obtained have been solved numerically on IBM 704 equipment for a number of simplified cases. It has been assumed that the beam is thin, and the electron trajectories in the absence of r-f effects are straight lines parallel to the circuit. These cases were chosen because, in the limit of linear interaction effects, the results can be compared with some of the analyses mentioned above. There is no fundamental problem involved in solving the equations for the general case; the main difficulty is simply one of computing time.

The present work is divided into four sections. In Chapter II, the model assumed is discussed, and a set of equations describing this model is derived and placed in a form suitable for numerical work. In Chapter III, the numerical techniques employed in the solution of these equations are described, and some of the difficulties encountered are pointed out. Chapter IV compares some of the solutions obtained here with the results presented in the papers mentioned above, and establishes the general validity of the equations. In Chapter V, the results of the nonlinear calculations are presented.

II. THE SYSTEM EQUATIONS

2.1 The Physical Model

The configuration of the model analyzed is illustrated in Fig. 6. This system consists of a slow-wave circuit located a distance d above a ground plane (the sole), the circuit having transitions to external transmission lines at z = 0 and z = L. The coordinate system is oriented so that the circuit is at y = d/2, and the sole at y = - d/2, and the circuit waves propagate in the z direction. Electromagnetic energy can be supplied or removed at either z = 0 or z = L to allow for either forward- or backward-wave interaction, and the phase velocity of a wave on the circuit is less than the velocity of light so that the electron beam can be made to travel at approximately the wave velocity. The electron beam is formed by a gun system to the left of z = 0 and is injected into the interaction region at any desired y position with any desired velocity (this means that the cathode potential is not necessarily the same as the sole potential). There is a static magnetic field $+B_o\hat{e}_x$ into the paper and a static electric field $-E_o\hat{e}_y$ so that in the absence of a circuit wave or space-charge interaction forces the electrons have an average drift velocity $u_o = E_o/B_o$ in the z direction. The beam is eventually collected on the circuit itself or on a collector to the right of z = L.

2.2 Assumptions

The main assumptions necessary to carry out this analysis are listed here. They are discussed more completely during the derivation of the equations.

1. All quantities are assumed to be independent of the x coordinate

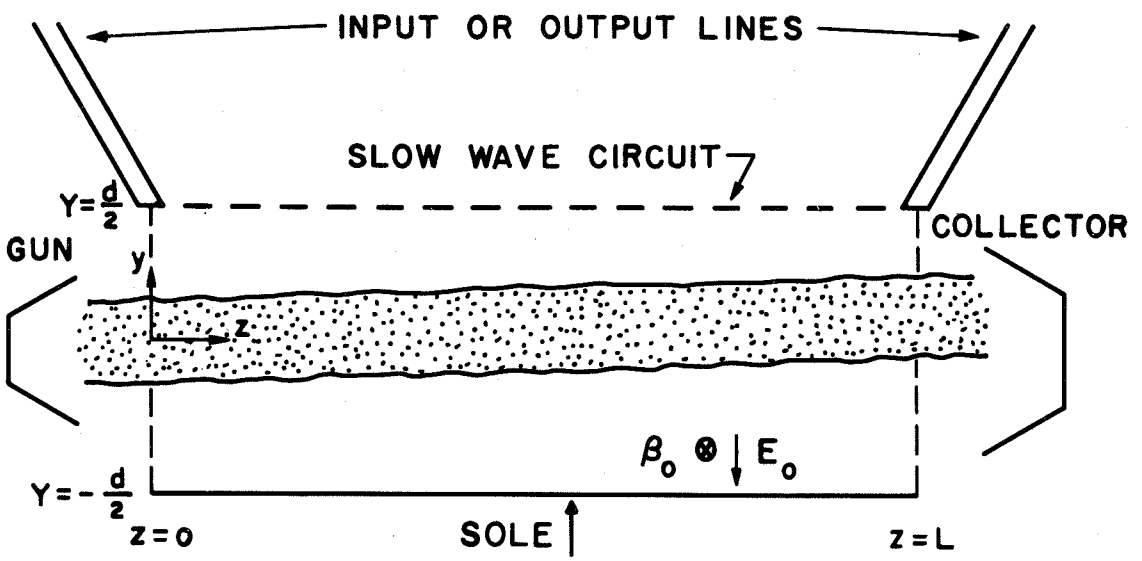

Fig. 6. The configuration of the system analyzed

over the width of the tube. There is no motion in the x-direction.

2. The solution will be a steady-state, periodic solution, i.e., all time-varying quantities repeat in a period $\omega t = 2\pi$. The problem can be solved by beginning with a set of conditions at $z = 0$ and integrating the equations with respect to z.

3. The actual slow-wave circuit is replaced by an equivalent, distributed-constant transmission line which propagates a wave with the velocity of the desired spatial harmonic component of a wave on the actual periodic structure. The impedance of the transmission line is so chosen that when the transmission line and the actual circuit are carrying the same power the electric field of the spatial harmonic is exactly equal to the field $E_z = - \partial V/\partial z$ given by the voltage on the equivalent transmission line.

4. The electron stream is treated as a finite number of charged particles. The stream is divided into a number of cylindrical volume elements, and these elements are replaced by an equivalent line charge or "electron" the motion of which is representative of the motion of all the charge in that element. This technique is used because the presence of electrons with different velocities at the same position in time and space, as can occur when there are electron crossovers in the beam, introduces no further complication into the analysis.

5. In computing the space-charge fields, the irregularities of the circuit are neglected. The space-charge interaction forces are computed by calculating the forces between the equivalent line charges when they are located between two parallel, conducting plates at $y = d/2$ and $y = -d/2$, one representing the circuit and one representing the sole.

6. The effect of the beam on the circuit wave is obtained by actually computing the displacement current flowing into the circuit because of the motion of the equivalent line charges.

7. In order to actually carry out Assumptions 5 and 6, it is necessary to know the positions of all the equivalent charges in the beam, but the positions are known only up to the last point of integration in z. It is assumed that the future positions of the charges can be predicted from a knowledge of velocity at the present positions.

8. It is assumed that only charge within a limited range of the point in question is effective in producing a field at that point. Numerical calculations for some typical geometries indicate that this is a valid assumption for ranges that are practical in terms of computation time. This result lends some strength to Assumption 7, since as the error in predicting the position of a charge increases, the effect of that charge decreases.

9. The force between two line charges approaches infinity as the line charges approach each other. In order to circumvent the difficulty which this situation introduces into the numerical work, it is assumed that the force between line charges drops suddenly to zero when the charges approach within a range ϵ of one another. This range is selected from numerical considerations. The neglect of the short-range force causes a reduction in the effective space-charge forces. A factor is introduced into the defined space-charge parameter to bring the results into agreement with small-signal theory.

10. Only one spatial harmonic component acts on the electron beam. This assumption is possible because, in general, the other spatial

harmonics are traveling at quite different velocities and produce no net effect on the beam.

11. Although the electron beam will, in general, contain harmonics, it is assumed that only the fundamental frequency component of voltage is present on the circuit, and that only the fundamental frequency component of beam current is effective in inducing fields on the circuit. The impedance of any wave at a harmonic of the fundamental frequency is generally much lower than the impedance of the fundamental, and the phase velocity of the harmonic would, in general, be quite different from that of the fundamental so that net interaction effects would be small even if there were a harmonic wave present. The same argument applies to the excitation of waves by the harmonics of the beam current.

12. The analysis is nonrelativistic, and the forces due to alternating magnetic fields are neglected since the magnetic forces are of the order of $(u_o/c)^2$ times the electric forces.

No assumptions are made about the state of the electron beam other than that it is injected into the interaction region from the left. The beam could be modulated, it could have a distribution of velocities, or it could be performing some kind of cycloidal motion. The beam can have width in the y direction, and different parts of the beam are acted on by the fields appropriate to the distance that the beam is away from the circuit.

The derivation of the equations is treated in three parts: the equations describing propagation on the circuit, the equations describing the motion of the electron beam, and those dealing with the

effects of the space-charge fields. The problem is first treated by using a straightforward choice of variables, and then a set of variables suitable for use in making numerical computations is introduced.

2.3 The Circuit Equation

The equation used to describe the circuit in this analysis is the familiar transmission-line equation for the voltage as a function of distance and time along a distributed-constant transmission line. The purpose of this section is to relate the constants of the transmission-line equation to the characteristics of the crossed-field device represented schematically in Fig. 6.

The equation for the voltage on a distributed-constant transmission line driven by a distributed current such as the one shown in Fig. 7 is

$$\frac{\partial^2 V}{\partial t^2} - \frac{1}{LC}\frac{\partial^2 V}{\partial z^2} = \sqrt{\frac{L}{C}}\,\frac{1}{\sqrt{LC}}\,\frac{\partial i}{\partial t} \qquad \text{(II. 1)}$$

where

$V(z, t)$ = the voltage across the line at any point

$i(z, t)$ = the current per unit length flowing into the line at any point

L = the inductance per unit length

C = the capacitance per unit length.

It has been assumed that the circuit is lossless; this assumption is merely for convenience; a finite value of R introduces only a slight complication in the numerical work. The constants $1/LC$ and L/C are chosen to relate the transmission line to the actual slow-wave circuit

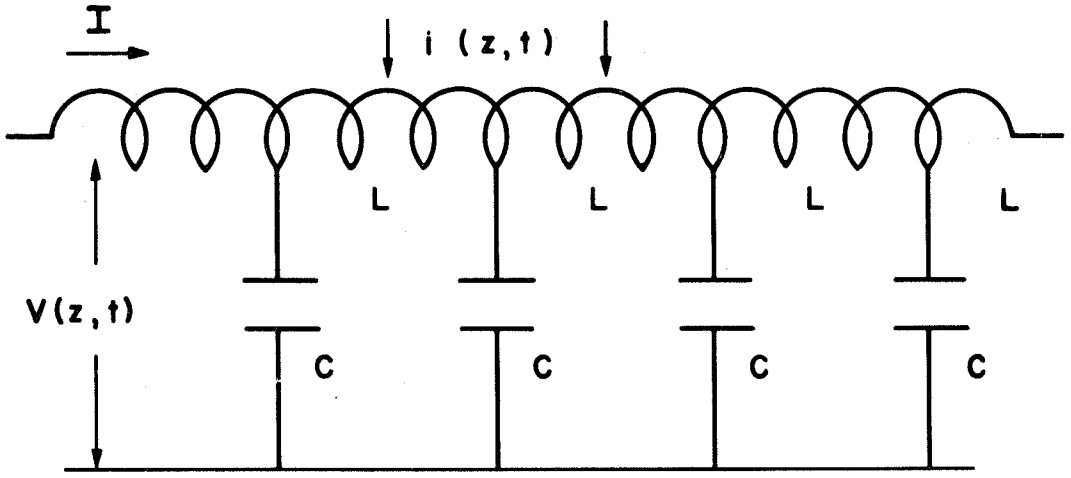

Fig. 7. A distributed constant transmission line driven by a distributed current

in much the same manner as is done in the small-signal analysis of the ordinary traveling-wave tube.[2] The quantity $1/LC$ is chosen equal to v_o^2 where v_o is the phase velocity of the desired spatial harmonic of a free wave on the actual periodic circuit. The homogeneous solution to equation II. 1 is then a voltage wave propagating with velocity v_o.

The choice of L/C is a little more complicated. It is clear that since equation II. 1 is a function of z and t only, it cannot describe the variations of the fields in the transverse direction. For a circuit propagating a slow wave in the z direction with propagation constant β and assumed to have no variations with x, the voltage can be shown to vary as $\sinh \beta y$ in the y direction (Appendix A). Since it is anticipated that the velocity of propagation of waves in the combined circuit and beam system will be near the average drift velocity of the electrons, it is assumed that the voltage variation as a function of y, z, and t is

$$V(y,z,t) = V(z,t)\ \frac{\sinh \beta_e (y + \frac{d}{2})}{\sinh \beta_e d} \qquad \text{(II. 2)}$$

where $\beta_e = \omega/u_o = \omega B_o/E_o$ is the propagation constant of a wave traveling at the electron drift velocity and $V(z,t)$ is a solution to equation II.1. The factor multiplying $V(z,t)$ in equation II. 2 is the appropriate variation of field with distance away from the circuit so that the characteristic impedance of the transmission line, $Z_o = \sqrt{L/C}$, must be chosen so that $E_z = -\partial V(z,t)/\partial z$ is exactly equal to the field, at $y = d/2$, of the desired spatial harmonic of the slow-wave circuit when the equivalent transmission line and the slow-wave circuit are carrying the same power. In the analysis of the ordinary traveling-wave tube, Z_o is

defined in terms of an average field over the region of the beam because it is assumed that the same field acts on all electrons at a particular position in z; in this case the correct field acts on all electrons. The average power carried by a distributed-constant transmission line in terms of the voltage on the circuit is $P_{ave.} = \left|V^2\right| /2Z_o$. Since $E_z = - \partial V(z,t)/\partial z$, for a free wave with propagation constant β the proper choice for Z_o is

$$Z_o = \frac{\left|V^2\right|}{2P_{ave.}} = \frac{\left|E_z^2\right|}{2\beta^2 P_{ave.}} \qquad \text{(II.3)}$$

where $\left|E_z\right|$ is the magnitude of E_z of the desired spatial harmonic evaluated at the edge of the circuit, $y = d/2$, when the slow-wave circuit is carrying $P_{ave.}$ with a propagation constant β. Equation II.1 can now be written

$$\frac{\partial^2 V}{\partial t^2} - v_o^2 \frac{\partial^2 V}{\partial z^2} = v_o Z_o \frac{\partial i}{\partial t} . \qquad \text{(II.4)}$$

The distributed current $i(z,t)$ driving the transmission line is the displacement current flowing into the line due to the motion of charges in the electron stream. The procedure for evaluating $i(z,t)$ in terms of the motion of the charge in the electron beam will be discussed in the section on space charge. The assumptions made in the Introduction regarding i will be reiterated. The characteristic impedance Z_o in equation II.4 is in reality a function of frequency for a periodic circuit. In general, it decreases for frequencies outside of the band for which the circuit was designed. In addition, the phase velocity of an

electromagnetic wave on a periodic circuit is also a function of frequency so that net interaction effects are small for frequencies other than those for which the velocity of wave propagation is approximately the same as the electron drift velocity. Because of these facts, although $\partial i/\partial t$ will, in general, contain harmonics, it is assumed that only the fundamental frequency component of voltage is present on the circuit and that only the fundamental frequency component of driving current is effective in equation II. 4.

The circuit equation becomes

$$\frac{\partial^2 V}{\partial t^2} - v_o^2 \frac{\partial^2 V}{\partial z^2} = \pm v_o Z_o \frac{\partial i_1}{\partial t} \qquad \text{(II.5)}$$

where i_1 has been written for the fundamental component of $i(z,t)$. The plus and minus signs have been included to allow for both forward- and backward-wave interaction; the plus sign for forward-wave interaction, and the minus sign for backward-wave interaction. The signs can be deduced from a consideration of an equivalent circuit of a backward-wave structure[2] or from a field analysis of an actual periodic circuit.[11]

2.4 The Equations of Motion

The general force equation for an electron moving in electric and magnetic fields is

$$m \frac{d^2 \bar{r}}{dt^2} = - |e| \bar{E} - |e| \frac{d\bar{r}}{dt} \times \bar{B} \qquad \text{(II.6)}$$

where

e = magnitude of the electronic charge

m = electronic mass

$\bar{r}$ = radius vector to the electron.

Equation II.6 can be separated into two equations in the y and z components since it has been assumed that there is no motion in the x direction.

$$\frac{d^2y}{dt^2} = -\eta E_y + \eta \frac{dz}{dt} B_x \tag{II.7}$$

$$\frac{d^2z}{dt^2} = -\eta E_z + \eta \frac{dy}{dt} B_x \tag{II.8}$$

where

$$\eta = \frac{e}{m} .$$

The electric field can now be separated into three parts: the field due to the energy on the circuit, the applied d-c field, and the field due to the combined effect of all the charges present. The fields due to the wave on the circuit can be obtained from the potential function defined in the preceding section.

$$E_y = -\frac{\partial V(y,z,t)}{\partial y} = -\beta_e V(z,t) \frac{\cosh \beta_e (y + \frac{d}{2})}{\sinh \beta_e d} \tag{II.9}$$

$$E_z = -\frac{\partial V(y,z,t)}{\partial z} = -\frac{\partial V(z,t)}{\partial z} \frac{\sinh \beta_e (y + \frac{d}{2})}{\sinh \beta_e d} \tag{II.10}$$

The applied d-c field is in the negative y direction only, $-E_o \hat{e}_y$.

The fields due to space charge will be denoted E_{sy} and E_{sz}. They will be determined explicitly in the next section. Since the a-c magnetic fields are neglected, the only magnetic field to be considered is the applied d-c magnetic field, $+B_o \hat{e}_x$. The equations of motion can now be written

$$\frac{d^2y}{dt^2} = +\eta\beta_e V(z,t) \frac{\cosh\beta_e(y+\frac{d}{2})}{\sinh\beta_e d} - \eta E_{sy} + \eta E_{oy} - \eta \frac{dz}{dt} B_{ox} \qquad \text{(II.11)}$$

$$\frac{d^2z}{dt^2} = \eta \frac{\partial V(z,t)}{\partial z} \frac{\sinh\beta_e(y+\frac{d}{2})}{\sinh\beta_e d} - \eta E_{sz} + \eta \frac{dy}{dt} B_{ox}. \qquad \text{(II.12)}$$

In the numerical solution of this problem the motion of each representative "electron" must be obtained; therefore equations (II.11) and (II.12) really represent 2N equations, where N is the number of "electrons" chosen to represent the beam.

2.5 The Effects of Space Charge

The fields due to space charge enter into both the circuit equation and the equations of motion. The fields produced by a line charge located between two infinite, conducting plates will be determined first. The relation between these fields and the fields due to the charge in the beam will then be obtained, and the terms due to space charge in the circuit equation (II.5) and the equations of motion (II.11) and (II.12) will be written out explicitly.

The electric field from an infinite line charge located between two infinite, conducting plates can be obtained by writing the expression for the potential of a line charge above a conducting plate and

performing a simple, conformal transformation to obtain the case of a line charge between two parallel conducting plates.[12] The problem could also be solved by images, but if more than two images are required for sufficient accuracy, the computing time involved is greater than the time required for the analytical expressions presented below. The fields at y and z due to a line charge q_ℓ at y' and z' are

$$E'_{sy} = \qquad \text{(II. 13)}$$

$$+\frac{q_\ell}{2\epsilon d}\left\{\frac{(\sin\frac{\pi y}{d}\cos\frac{\pi y'}{d})\left[\sin\frac{\pi y'}{d}\sin\frac{\pi y}{d}+\cosh\frac{\pi}{d}(z-z')\right]-\sin\frac{\pi y'}{d}\cos\frac{\pi y'}{d}\cos^2\frac{\pi y}{d}}{-\left[-\sin\frac{\pi y'}{d}\sin\frac{\pi y}{d}+\cosh\frac{\pi}{d}(z-z')\right]^2-\cos^2\frac{\pi y'}{d}\cos^2\frac{\pi y}{d}}\right\}$$

$$E'_{sz} = \frac{q_\ell}{2\epsilon d}\left\{\frac{\cos\frac{\pi y'}{d}\cos\frac{\pi y}{d}\sinh\frac{\pi}{d}(z-z')}{\left[-\sin\frac{\pi y'}{d}\sin\frac{\pi y}{d}+\cosh\frac{\pi}{d}(z-z')\right]^2-\cos^2\frac{\pi y'}{d}\cos^2\frac{\pi y}{d}}\right\}. \qquad \text{(II. 14)}$$

The conducting plates are located at $y = d/2$ and $y = -d/2$, and the line charge is parallel to the x axis.

The fields due to a cylindrical volume of charge $\rho dy'dz'$, located at y', z', are assumed to be the fields calculated from equations II. 13 and II. 14 with $q_\ell = \rho\, dy'\, dz'$. This approximation is good as long as the point of interest y, z is far enough away from the circuit so that the irregularities of the surface are unimportant and as long as $(z - z') > dz'/2$ and $(y - y') > dy'/2$ since the fields external to a circular cylinder of charge are exactly the same as if all the charge were

concentrated on the axis of the cylinder. When (z - z') and (y - y') approach zero, equation II. 13 and II. 14 approach infinity. This does not represent the physical situation accurately; some artifice must be used to eliminate this infinity. The technique actually used is to make the short-range fields be zero out to some fairly arbitrary distance and then suddenly let the fields be those of the line charge: a space-charge correction factor is then determined to account for the fields excluded.

Since the difficulty just discussed is associated with the finite size of the elements dy' and dz', it introduces no complication into the derivation of the equations. It will be discussed further in the section concerned with the numerical solution of the equations.

With the aid of equation II. 13, it is now possible to determine the driving term $\partial i_1/\partial t$ of the circuit equation in terms of an integral over the charge in the electron stream. The total displacement current flowing into the circuit at z due to the charge in the beam is

$$\frac{\partial i}{\partial t}(z,t) = w \frac{\partial^2}{\partial t^2} D_y\left(\frac{d}{2}, z, t\right) \qquad \text{(II. 15)}$$

where $D_y(\frac{d}{2}, z, t)$ is the displacement flux terminating on the circuit at z, and w is the width of the actual circuit in the x direction. From equation II. 13

$$d\left[D_y\left(\frac{d}{2}, z, t\right)\right] = \frac{\rho(y', z', t)}{2d} \frac{\cos\frac{\pi}{2} y'}{-\sin\frac{\pi}{2} y' + \cosh\frac{\pi}{d}(z - z')} dz'dy',$$

(II. 16)

and defining

$$F = \frac{\cos \frac{\pi}{d} y'}{-\sin \frac{\pi y'}{d} + \cosh \frac{\pi}{d} (z - z')} , \tag{II.17}$$

$$\left[\frac{w \partial^2 D_y(\frac{d}{2}, y, t)}{\partial t^2}\right]_1 = \left[\frac{w}{2d} \frac{\partial^2}{\partial t^2} \int_{-\infty}^{\infty} \int_{-d/2}^{d/2} \rho(y', z', t) F \, dy' dz'\right]_1 \tag{II.18}$$

Retardation effects have been neglected in writing equation II.18; the flux at $\frac{d}{2}, z$ is assumed to have propagated instantaneously from y', z'. This assumption is permissible because the wave velocity and the electron velocity are much less than the velocity of light and because the function F decreases rapidly with increase in $(z - z')$ so that as the effect of retardation becomes more important, the strength of the retarded fields becomes less. The subscript 1 on the brackets of equation II.18 indicates that the fundamental frequency component of this equation is to be taken in accordance with the assumptions made in obtaining the circuit equation. The equation for the circuit voltage can now be written

$$\frac{\partial^2 V}{\partial t^2} - v_o^2 \frac{\partial^2 V}{\partial z^2} = \pm \frac{v_o Z_o w}{2d} \left[\frac{\partial^2}{\partial t^2} \int_{-\infty}^{\infty} \int_{-d/2}^{d/2} \rho(y', z', t) \, F \, dy' dz'\right]_1 \tag{II.19}$$

The expressions for the space-charge fields E_{sy} and E_{sz} of equations II.11 and II.12 can be obtained in a similar fashion. Define

$$Y = \left\{ \frac{\left[\sin\frac{\pi y}{d}\cos\frac{\pi y'}{d}\right]\left[-\sin\frac{\pi y'}{d}\sin\frac{\pi y}{d} + \cosh\frac{\pi}{d}(z - z')\right] - \sin\frac{\pi y'}{d}\cos\frac{\pi y'}{d}\cos^2\frac{\pi y}{d}}{\left[-\sin\frac{\pi y}{d}\sin\frac{\pi y'}{d} + \cosh\frac{\pi}{d}(z - z')\right]^2 - \cos^2\frac{\pi y'}{d}\cos^2\frac{\pi y}{d}} \right\} \tag{II.20}$$

and

$$Z = \frac{\cos\frac{\pi y'}{d}\cos\frac{\pi y}{d}\sinh\frac{\pi}{d}(z - z')}{\left[-\sin\frac{\pi y}{d}\sin\frac{\pi y'}{d} + \cosh\frac{\pi}{d}(z - z')\right]^2 - \cos^2\frac{\pi y'}{d}\cos^2\frac{\pi y}{d}}. \tag{II.21}$$

Then

$$E_{sy}(y, z, t) = \frac{1}{2\epsilon d}\int_{-\infty}^{\infty}\int_{-d/2}^{d/2} \rho(y', z', t)\, Y\, dy'dz' \tag{II.22}$$

and

$$E_{sz}(y, z, t) = \frac{1}{2\epsilon d}\int_{-\infty}^{\infty}\int_{-d/2}^{d/2} \rho(y', z', t)\, Z\, dy'dz' \ . \tag{II.23}$$

The fact that it is possible to have electron crossovers in a nonlinear problem of this type means that the electron stream can no longer be treated as a fluid; the Lagrange rather than the Eulerian equation of continuity must be used. The Lagrange equation of continuity in two dimensions is

$$\rho_o(y_o, z_o, 0)\, dy_o dz_o = \rho(y, z, t)\, dy\, dz \ . \tag{II.24}$$

This equation simply states that all the charge initially in the region $dy_o dz_o$ at $y_o, z_o, 0$ is contained in the region $dy\,dz$ at y, z, t. If the electrons at the corners of the element $dy_o dz_o$ end on the corners of the element $dy\,dz$ after a time t, then the total charge in the element $dy_o dz_o$ must be the same as the total charge in the element $dy\,dz$. The area elements can be related to give

$$\rho(y, z, t) = \rho_o(y_o, z_o, 0) \begin{vmatrix} \frac{\partial y_o}{\partial y} & \frac{\partial y_o}{\partial z} \\ \frac{\partial z_o}{\partial y} & \frac{\partial z_o}{\partial z} \end{vmatrix} \tag{II.25}$$

In order to apply equation II.25, the trajectory equations for a representative set of electrons must be known; that is, y and z must be known as a function of time for the particular electron that was at y_o, z_o at $t = 0$.

$$y = y(y_o, z_o, t) \tag{II.26}$$

$$z = z(y_o, z_o, t) \tag{II.27}$$

These are exactly the quantities that are obtained from integration of the force equations.

There is a complication in the use of equation II.25 when there are electron crossovers. y_o and z_o are not single-valued functions of y and z, and the right-hand side of equation II.25 should be written as a sum over the different branches of the functions. Rather than use equation II.25 and integrate over y' and z', however, it is easier to use equation II.24 and convert the integrals in equations II.19, II.22, and II.23 into integrals over the initial positions and then use equations II.26 and II.27 to convert F, Y, and Z into functions of the initial positions, because y and z are always single-valued functions of y_o and z_o. Equations II.19, II.22, and II.23 become

$$\frac{\partial^2 V}{\partial z^2} - \frac{1}{v_o^2} \frac{\partial^2 V}{\partial t^2} = \mp \frac{Z_o w}{2dv_o} \left[\frac{\partial^2}{\partial t^2} \int_{-\infty}^{\infty} \int_{-d/2}^{d/2} \rho_o(y'_o, z'_o, 0)\, F\, dy'_o\, dz'_o \right]_1 \tag{II.28}$$

$$E_{sy}(y,z,t) = \frac{1}{2\epsilon d}\int_{-\infty}^{\infty}\int_{-d/2}^{d/2} \rho_o(y'_o, z'_o, 0)\, Y\, dy'_o\, dz'_o \qquad \text{(II.29)}$$

$$E_{sz}(y,z,t) = \frac{1}{2\epsilon d}\int_{-\infty}^{\infty}\int_{-d/2}^{d/2} \rho_o(y'_o, z'_o, 0)\, Z\, dy'_o\, dz'_o \qquad \text{(II.30)}$$

Equations II.11, II.12, and II.28 together with equations II.29 and II.30 are the equations describing the system.

2.6 The System Equations in Reduced Variables

The choice of variables used to describe the problem has been straightforward. Since these variables are not a practical choice for numerical work, a set of reduced variables has been chosen to simplify the numerical computations and to eliminate duplications in the work. These variables have been chosen to give agreement with the small-signal analyses of crossed-field devices as much as possible. Other variables have been chosen similar to the variables of the large-signal analysis of the ordinary traveling-wave tube. The variables are listed here with some of the reasons for their choice. The system equations are then written in terms of the new variables.

The voltage on the circuit is assumed to be of the form

$$V(y,z,t) = A(z)\sinh\beta_e\left(y+\frac{d}{2}\right)\frac{2I_oZ_o\Phi^2}{D}\cos\phi(z,t)$$

$$= KA(z)\frac{\sinh\beta_e\left(y+\frac{d}{2}\right)}{\sinh\beta_e d}\cos\phi \quad . \qquad \text{(II.31)}$$

where

$$K = \frac{2I_oZ_o\Phi^2}{D}\sinh\beta_e d \quad .$$

A(z) is the amplitude function and it is assumed to vary slowly with z. I_o is the total current in the unperturbed electron beam defined as a positive number. Z_o is defined by equation II.3, and D is defined by the equation

$$D^2 = \frac{\omega}{\omega_c} \frac{I_o Z_o \bar{\Phi}^2}{2V_o} a \; ; \tag{II.32}$$

the small-signal gain of a crossed-field tube is proportional to D. V_o is a voltage corresponding to the energy of the electrons at the average drift velocity;

$$V_o = \frac{u_o^2}{2\eta} = \frac{1}{2\eta} \frac{E_o^2}{B_o^2} \; . \tag{II.33}$$

$\bar{\Phi}$ is a factor which relates the impedance at the beam entrance position to the impedance at the circuit;

$$Z(y_o) = Z_o \frac{\sinh^2 \beta_e (y_o + \frac{d}{2})}{\sinh^2 \beta_e d} = Z_o \bar{\Phi}^2 . \tag{II.34}$$

a is the magnitude of the ratio of the r-f electric field in the y direction to that in the z direction at the beam entrance position y_o.

$$a = \left| \frac{E_y(y_o)}{E_z(y_o)} \right| = \coth \beta_e d (y_o + \frac{d}{2}) \; . \tag{II.35}$$

ω_c is the cyclotron angular frequency;

$$\omega_c = \eta B_o \; . \tag{II.36}$$

The phase of the voltage wave

$$\phi(z,t) \equiv \omega(\frac{z}{u_o} - t) - \theta(z) \tag{II.37}$$

defines $\theta(z)$ as the negative of the difference between the actual phase of the wave and the phase of a wave traveling with a velocity equal to the average drift velocity of the electrons. It is anticipated that θ will be a slowly varying function of z. A direct consequence of equation II.37 is

$$\left.\frac{\partial}{\partial t}\right|_z = -\omega \left.\frac{\partial}{\partial \phi}\right|_z . \tag{II.38}$$

The normalized y and z coordinates are

$$r = \frac{\pi y}{d} \tag{II.39}$$

and

$$s = D\,\beta_e z \ . \tag{II.40}$$

ϕ_o^i is the phase of the circuit wave that the i^{th} "electron" sees when it is at $z = 0$, and r_o^i is the normalized y position of the i^{th} electron when it is at $z = 0$.

$$\phi_o = \frac{\omega z_o}{u_1(y)} \tag{II.41}$$

where $u_1(y)$ is the z velocity of the electrons as they enter the interaction region. Equation II.37 can be written

$$z^i = \frac{u_o}{\omega}\left[\phi(s, r_o^i, \phi_o^i) + \theta(s)\right] + u_o t^i \ ; \tag{II.42}$$

in this form it represents the z position of the i^{th} electron in terms of the phase of the voltage wave on the circuit as seen by the i^{th} electron when it is at z. The equations

$$\frac{dy^i}{dt} \equiv 2u_o\, Dp^i(r_o^i, s, \phi_o^i) \tag{II.43}$$

and

$$\frac{dz^i}{dt} \equiv u_o \left[1 + 2Dq^i(r_o^i, s, \phi_o^i)\right] \tag{II.44}$$

define the velocity components of the electrons. When a quantity is written as a function of r_o^i, s, ϕ_o^i, as in some of the preceding equations, it simply means that at some position s these quantities are different for electrons that started in different phases and at different r positions.

Equations II.34 and II.41 can be used to convert the left-hand side of equation II.24 to

$$\rho_o(y_o, z_o, 0)\left|dy_o\, dz_o\right| = \frac{d}{\pi\omega} u_1(y_o)\, \rho_o(y_o, 0, \phi_o)\left|dr_o\, d\phi_o\right|. \tag{II.45}$$

$u_1(y_o)\, \rho_o(y_o, 0, \phi_o)$ must be independent of ϕ_o since the stream is unmodulated at z = 0. Let

$$i_1 = \left|u_1(y_o)\, \rho_o(y_o)\right| \tag{II.46}$$

be the current density in the unmodulated electron stream and let

$$i_2 = I_o/\tau w \tag{II.47}$$

be the average current density in the unmodulated electron stream. τ is the beam thickness in the y direction at z = 0 and w is the beam-width in the x direction. The quantity

$$\rho_1 = \frac{i_2}{u_o} \tag{II.48}$$

is a sort of average charge density in the electron stream and

$$\omega_p^2 = \left|\frac{\eta\rho_1}{\epsilon_o}\right| \tag{II.49}$$

is a plasma frequency. A space-charge parameter

$$g = \frac{\omega_p^2}{8\omega\omega_c D} \tag{II.50}$$

is defined similar to those used by Tien[9] and Rowe[10] in the large-signal analysis of the ordinary traveling-wave tube and is easily related to the parameter used by Gould[5] in the small-signal analysis of beam-type, crossed-field devices. The expression

$$u_o = v_o(1 + Db) \tag{II.51}$$

defines a velocity injection parameter b, similar to that used by Pierce and others in various traveling-wave-tube analyses. The quantity u_o in equation II.51 is the average drift velocity of the electrons in the absence of space-charge effects; the actual injection velocities are specified by the initial values of p^i and q^i.

2.7 The Circuit Equation in Reduced Variables

With the aid of equation II.38, the equation for the circuit voltage can be written

$$\frac{\partial^2 V(z,t)}{\partial z^2} - \frac{\omega^2}{v_o^2}\frac{\partial^2 V(z,t)}{\partial \phi^2} = \mp \frac{\omega^2 w Z_o}{2v_o d}\frac{\partial^2}{\partial \phi^2}\int_{-\infty}^{\infty}\int_{-d/2}^{d/2} \rho_o(y_o', z_o') F\, dy_o' dz_o'. \tag{II.52}$$

Equation II.31 defining the circuit voltage can be used to rewrite the terms on the left-hand side of equation II.52.

$$\frac{\partial V}{\partial z} = KD\beta_e\left\{\frac{dA}{ds}\cos\phi - A\sin\phi\frac{\partial\phi}{\partial s}\right\} \tag{II.53}$$

$$\frac{\partial\phi}{\partial s} = \frac{1}{D} - \frac{d\theta}{ds} \tag{II.54}$$

$$\frac{\partial^2 V}{\partial z^2} = (D\beta_e)^2 K\left\{\frac{d^2}{ds^2}\cos\phi - \frac{2dA}{ds}\sin\phi\frac{\partial\phi}{\partial s} - A\cos\phi\left(\frac{\partial\phi}{\partial s}\right)^2 - A\sin\phi\frac{\partial^2\phi}{\partial s^2}\right\}. \tag{II.55}$$

$$\frac{\partial^2 V}{\partial\phi^2} = -AK\cos\phi\ . \tag{II.56}$$

The right-hand side of equation II.52 can be expanded in a Fourier series in ϕ since, for constant z, ϕ is directly proportional to t. If only the fundamental component of this expansion is retained, the right-hand side of equation II.52 becomes

$$\pm\frac{\omega^2 w Z_o}{2\pi v_o d}\left[\left\{\int_0^{2\pi}\int_{-\infty}^{\infty}\int_{-d/2}^{d/2}\rho_o F\, dy'_o\, dz'_o\cos\phi'(z,t)\, d\phi'\right\}\cos\phi\right.$$
$$\left.+\left\{\int_0^{2\pi}\int_{-\infty}^{\infty}\int_{-d/2}^{d/2}\rho_o F\, dy'_o\, dz'_o\sin\phi'(z,t)\, d\phi'\right\}\sin\phi\right] \tag{II.57}$$

The functions $\sin\phi'$ and $\cos\phi'$ have been written outside of the y'_o, z'_o integrals because ϕ' is not a function of y'_o or z'_o. Since $\sin\phi$ and $\cos\phi$ are orthogonal functions, the coefficients multiplying $\sin\phi$ and $\cos\phi$ in the circuit equation can be equated individually, thereby yielding two equations for the circuit.

$$(D\beta_e)^2 K\left\{\frac{d^2A}{ds^2} - A\left(\frac{1}{D} - \frac{d\theta}{ds}\right)^2\right\} + AK\frac{\omega^2}{v_o^2} =$$

$$\pm\frac{\omega^2 w Z_o}{2\pi v_o d}\int_0^{2\pi}\int_{-\infty}^{\infty}\int_{-d/2}^{d/2}\rho_o F\, dy'_o\, dz'_o\cos\phi'\, d\phi' \tag{II.58}$$

$$(D\beta_e)^2 K\left\{A\frac{d^2\theta}{ds^2} - 2\frac{dA}{ds}\left(\frac{1}{D} - \frac{d\theta}{ds}\right)\right\} =$$

$$\pm \frac{\omega^2 w Z_o}{2\pi v_o d}\int_0^{2\pi}\int_{-\infty}^{\infty}\int_{-d/2}^{d/2}\rho_o F\, dy'_o\, dz'_o \sin\phi' d\phi'. \qquad \text{(II.59)}$$

Equation II.51 defining the velocity injection parameter b can be used to reduce equations II.58 and II.59 to

$$\frac{d^2A}{ds^2} - A\left[\left(\frac{1}{D} - \frac{d\theta}{ds}\right)^2 - \left(\frac{1 + Db}{D}\right)^2\right] =$$

$$\pm \left(\frac{1 + Db}{D}\right)\frac{u_o w}{d4\pi I_o \Phi^2 \sinh\beta_e d}\int_0^{2\pi}\int_{-\infty}^{\infty}\int_{-d/2}^{d/2}\rho_o F\, dy'_o dz'_o \cos\phi' d\phi' \qquad \text{(II.60)}$$

$$A\frac{d^2\theta}{ds^2} - 2\frac{dA}{ds}\left(\frac{1}{D} - \frac{d\theta}{ds}\right) =$$

$$\pm \left(\frac{1 + Db}{D}\right)\frac{u_o w}{d4\pi I_o \Phi^2 \sinh\beta_e d}\int_0^{2\pi}\int_{-\infty}^{\infty}\int_{-d/2}^{d/2}\rho_o F\, dy'_o dz'_o \sin\phi' d\phi'. \qquad \text{(II.61)}$$

Equations II.39, II.40, II.46, and II.47 can be used to convert the right-hand sides of equations II.60 and II.61 to integrals over ϕ'_o and r'_o.

$$\frac{d^2A}{ds^2} - A\left[\left(\frac{1}{D} - \frac{d\theta}{ds}\right)^2\right] - \left(\frac{1 + Db}{D}\right)^2 =$$

$$\pm \left(\frac{1 + Db}{D}\right)\frac{1}{4\pi^2 \Phi^2 \sinh\beta_e d\beta_e \tau}\int_0^{2\pi}\int_{\phi'_o - \pi}^{\phi'_o + \pi}\int_{-1}^{1}\frac{i_1}{i_2} F dr'_o d\phi'_o \cos\phi' d\phi' \qquad \text{(II.62)}$$

$$A\frac{d^2\theta}{ds^2} - 2\frac{dA}{ds}\left(\frac{1}{D} - \frac{d\theta}{ds}\right) =$$

$$\mp\left(\frac{1+Db}{D}\right)\frac{1}{4\pi^2\Phi^2\sinh\beta_e d\beta_e\tau}\int_0^{2\pi}\int_{\phi_o'-\pi}^{\phi_o'+\pi}\int_{-1}^{1}\frac{i_1}{i_2}F\,dr_o'\,d\phi_o'\sin\phi' d\phi' \qquad \text{(II.63)}$$

Equations II.62 and II.63 are the circuit equations in reduced variables. The range of the integral in ϕ_o' has been changed from $-\infty$ to ∞ to $\phi_o' - \pi$ to $\phi_o' + \pi$. That is, only charge that started within phase $\pm\pi$ of the charge that is at z at time t is effective in producing a field at z. After the beam is bunched, the electrons may not be in the same order as at starting, so that in the numerical work the integral is carried out to include those electrons which are actually nearest to the electron of interest. This will be discussed in the section concerning numerical solutions. Chopping off the integral is an assumption that is based on the fact that F is a rapidly decreasing function of $z - z'$. The same assumption will be made for the integrals involving Y and Z.

2.8 The Equations of Motion in Reduced Variables

The equations of motion, II.11 and II.12, can now be written in terms of the new variables. The acceleration in the y direction is

$$\frac{d}{dt}\left(\frac{dy}{dt}\right) = \frac{ds}{dt}\frac{\partial}{\partial s}\left(\frac{dy}{dt}\right) = 2\beta_e D^2 u_o^2\left[1 + 2Dq\right]\frac{\partial p}{\partial s}, \qquad \text{(II.64)}$$

and the acceleration in the z direction is

$$\frac{d}{dt}\left(\frac{dz}{dt}\right) = \frac{ds}{dt}\frac{\partial}{\partial s}\left(\frac{dz}{dt}\right) = 2\beta_e D^2 u_o^2\left[1 + 2Dq\right]\frac{\partial q}{\partial s}. \qquad \text{(II.65)}$$

Equations II.11 and II.12 become

$$2\beta_e D^2 u_o^2 \left[1 + 2Dq\right] \frac{\partial p}{\partial s} = \eta\beta_e KA \frac{\cosh \beta_e (y + \frac{d}{2})}{\sinh \beta_e d} \cos\phi$$

$$+ \eta E_o - \eta B_o u_o \left[1 + 2Dq\right] - \frac{\eta}{2\epsilon d} \int_{-\infty}^{\infty} \int_{-d/2}^{d/2} \rho_o Y \, dy'_o \, dz'_o \qquad \text{(II.66)}$$

and

$$2\beta_e D^2 u_o^2 \left[1 + 2Dq\right] \frac{\partial q}{\partial s} = K\beta_e d \frac{\sinh \beta_e (y + \frac{d}{2})}{\sinh \beta_e d} \left\{ \frac{dA}{ds} \cos\phi - A \sin\phi \left[\frac{1}{D} - \frac{d\theta}{ds} \right] \right\} \qquad \text{(II.67)}$$

Equations II.66 and II.67 can be reduced to

$$\left[1 + 2Dq\right] \frac{\partial p}{\partial s} = \qquad \text{(II.68)}$$

$$\frac{\omega_c}{D\omega} \left[\frac{A}{a} \cosh \frac{\beta_e d}{2} (1 + r) \cos\phi - q + \frac{2g}{\pi} \int_{\phi'_o - \pi}^{\phi'_o + \pi} \int_{-1}^{1} \frac{i_1}{i_2} Y \, dr'_o \, d\phi'_o \right]$$

$$\left[1 + 2Dq\right] \frac{\partial q}{\partial s} =$$

$$\frac{\omega_c}{D\omega} \left[\left\{ \frac{dA}{ds} \cos\phi - A \sin\phi \left(\frac{1}{D} - \frac{d\theta}{ds} \right) \right\} \frac{D}{a} \sinh \frac{\beta_e d}{2} (1 + r) + p + \right. \qquad \text{(II.69)}$$

$$\left. \frac{2g}{\pi} \int_{\phi'_o - \pi}^{\phi'_o + \pi} \int_{-1}^{1} \frac{i_1}{i_2} Z \, dr'_o \, d\phi'_o \right] .$$

It should be recognized that p, q, r, and ϕ in equations II.68 and II.69 are functions of s, r_o, and ϕ_o. In the integral terms, i_1 is a function of r'_o; i_2 is a constant, and Y and Z are functions of r_o, r'_o, ϕ_o, ϕ', and s.

Two additional equations are necessary to complete the problem, equations relating r and ϕ to the velocities. By definition, $dy/dt = 2u_o Dp$, and for a particular electron,

$$\frac{dy}{dt} = \frac{ds}{dt} \frac{\partial y}{\partial s} = D\omega \left[1 + 2Dq\right] \frac{\partial y}{\partial s} \qquad \text{(II.70)}$$

Therefore,

$$\frac{\partial r}{\partial s} = \frac{2\pi}{\beta_e d} \frac{p}{[1 + 2Dq]} \quad . \tag{II.71}$$

The equation for ϕ is obtained by taking the time derivative of equation II.42 and setting it equal to equation II.44.

$$\frac{dz}{dt} = \frac{u_o}{\omega} \left[\frac{ds}{dt} \left(\frac{\partial \phi}{\partial s} + \frac{d\theta}{ds} \right) \right] + u_o = \frac{1}{\beta_e D} \left(\frac{ds}{dt} \right)$$

$$\frac{\partial \phi}{\partial s} + \frac{d\theta}{ds} = \frac{2q}{1 + 2Dq} \quad . \tag{II.72}$$

Equations II.62, II.63, II.68, II.69, II.71, and II.72 comprise the general working equations for a beam-type, crossed-field device.

2.9 The System Equations for Small D

If $D \ll 1$ so that terms of first order and higher in D can be neglected, the equations above reduce to

$$\frac{d\theta}{ds} + b = \mp \frac{1}{8\pi^2 A \mathbb{I}^2 \sinh \beta_e d \beta_e \tau} \int_0^{2\pi} \int_{\phi'_o - \pi}^{\phi'_o + \pi} \int_{-1}^{1} \frac{i_1}{i_2} F \, dr'_o \, d\phi'_o \cos\phi \, d\phi \tag{II.73}$$

$$\frac{dA}{ds} = \pm \frac{1}{8\pi^2 \mathbb{I}^2 \sinh \beta_e d \beta_e \tau} \int_0^{2\pi} \int_{\phi'_o - \pi}^{\phi'_o + \pi} \int_{-1}^{1} \frac{i_1}{i_2} F \, dr'_o \, d\phi'_o \sin\phi \, d\phi \tag{II.74}$$

$$\left[1 + 2Dq\right] \frac{\partial p}{\partial s} = \frac{\omega_c}{D\omega} \left[\frac{A}{a} \cosh \frac{\beta_e d}{2} (1 + r) \cos\phi - q + \frac{2g}{\pi} \int_{\phi'_o - \pi}^{\phi'_o + \pi} \int_{-1}^{1} \frac{i_1}{i_2} Y \, dr'_o \, d\phi'_o \right] \tag{II.75}$$

$$\left[1 + 2Dq\right]\frac{\partial q}{\partial s} = \frac{\omega_c}{D\omega}\left[\frac{A}{a}\cosh\frac{\beta_e d}{2}(1+r)\sin\phi + p + \frac{2g}{\pi}\int_{\phi'_o - \pi}^{\phi'_o - \pi}\int_{-1}^{1}\frac{i_1}{i_2} Z\, dr'_o d\phi'_o\right] \tag{II.76}$$

$$\frac{\partial r}{\partial s} = \frac{2\pi}{\beta_e d}\,\frac{p}{\left[1 + 2Dq\right]} \tag{II.77}$$

$$\frac{\partial \phi}{\partial s} + \frac{d\theta}{ds} = \frac{2q}{1 + 2Dq} \tag{II.78}$$

The terms containing p and q multiplied by D have been retained in these equations because it is possible for these terms to be large even if D is small, if the electrons are poorly injected into the focusing fields.

2.10 The Thin-Beam Equations

The case for which the beam thickness in the transverse direction is so small that all electrons at a given z position are acted on by the same fields has received considerable attention in the small-signal case.[1], [2], [3], [5], [6] If the electron stream can be considered thin so that the integral in r_o reduces to multiplication by a constant, $i_1 = i_2$ and $dr'_o = \pi\tau/d$, the equations for small D reduce to

$$\frac{d\theta}{ds} + b = \mp\frac{1}{8\pi\beta_e d\bar{\Phi}^2 \sinh\beta_e d A}\int_0^{2\pi}\int_{\phi'_o - \pi}^{\phi'_o + \pi} F\, d\phi'_o \cos\phi' d\phi' \tag{II.79}$$

$$\frac{dA}{ds} = \pm\frac{1}{8\pi\beta_e d\bar{\Phi}^2 \sinh\beta_e d}\int_0^{2\pi}\int_{\phi'_o - \pi}^{\phi'_o + \pi} F\, d\phi'_o \sin\phi' d\phi' \tag{II.80}$$

$$\left[1 + 2Dq\right]\frac{\partial p}{\partial s} = \frac{\omega_c}{D\omega}\left[\frac{A}{a}\cosh\frac{\beta_e d}{2}(1+\frac{2}{\pi}r)\cos\phi - q + \frac{S}{2\beta_e d}\int_{\phi'_o - \pi}^{\phi'_o + \pi} Y\, d\phi'_o\right] \tag{II.81}$$

$$\left[1 + 2Dq\right] \frac{\partial q}{\partial s} = \frac{\omega_c}{D\omega} \left[- \frac{A}{a} \sinh \frac{\beta_e d}{2} (1 + r) \sin \phi + p + \frac{S}{2\beta_e d} \int_{\phi'_o - \pi}^{\phi'_o + \pi} Z \, d\phi'_o \right] \tag{II.82}$$

$$\frac{\partial r}{\partial s} = \frac{2\pi}{\beta_e d} \frac{p}{1 + 2Dq} \tag{II.83}$$

$$\frac{\partial \phi}{\partial s} + \frac{d\theta}{ds} = \frac{2q}{1 + 2Dq} \tag{II.84}$$

The constant S in equations II.81 and II.82 has been defined to be similar to that used by Gould.[6]

$$S = \frac{\sigma_o}{2\epsilon_o B_o u_o D} \tag{II.85}$$

where $\sigma_o = I_o/u_o w$ is a surface-charge density. S is a space-charge parameter that is typically of the order of 0.5 to 3. $\beta_e DS$ is actually the gain constant for the growth of space-charge waves on a thin beam of electrons mid-way between two flat, conducting plates.

The equations derived here describe the beam-type, crossed-field, traveling-wave tube in a quite general manner. The choice of reduced variables is arbitrary in most cases, and to become familiar with the variables is no insignificant task. The computational results will be presented in a fashion that will not require a detailed knowledge of the variables.

III. NUMERICAL SOLUTION OF THE SYSTEM EQUATIONS

The equations as derived in the preceding chapter are specifically designed for solution on a high-speed digital computer. The complexity of the space-charge functions and the number of electrons necessary to obtain reasonable accuracy in the cases in which space-charge is included are such that only a large-scale machine is practical. The solutions were actually carried out on IBM 704 equipment. This chapter will describe in detail the procedure for solving the small-D, thin-beam equations numerically. Although the discussion is restricted to this particular case, with minor modifications the method applies to the more general cases. The equations will first be written in finite difference form. The general procedure for solving the equations will then be discussed and a specific format set down. Finally, a brief discussion of the errors and the amount of computing time involved will be given.

3.1 The Small-D, Thin-Beam Equations in Finite Difference Form

The small-D, thin-beam equations II.79, II.80, II.81, II.82, II.83, and II.84 must be converted to equations relating a finite number of points in order for the problem to be programmed for a digital computer. The finite difference forms selected were chosen for their simplicity rather than for extreme accuracy for two reasons. The chief reason is that more storage space and more computing time are required for the more refined techniques. Admittedly, more accurate approximations would allow the integration interval to be larger and thus reduce the computing time, but there is still the storage-space

requirement. This problem was first coded for a Univac Scientific Computer with only 1024 words of high-speed storage, and a fair share of the computing time was used in transferring between low-speed and high-speed storage. On the IBM 704, the entire problem can be carried in the high-speed storage, and the storage problem is not particularly acute, at least for the thin-beam case. The second reason for selecting simple difference forms in the space-charge terms is that the approximations regarding the near and far fields are so severe that refining the numerical techniques for the rest of the terms is unwarranted.

It has been pointed out previously that the terms involving Dp and Dq in the small-D equations have been retained to allow for cases in which the electron trajectories would not be straight lines in the absence of circuit and space-charge fields. The discussion will now be confined to cases where it can be assumed that Dp and Dq are negligible compared with unity.

A few more definitions must be introduced before the equations can be written in finite difference form. The equations are to be integrated with respect to s; the integration interval in s and the integration step are defined by

$$s = mh; \quad m = 0, 1, 2, 3 \ldots; \quad h = \text{constant}. \tag{III.1}$$

A subscript m on any quantity means that quantity evaluated at $s = mh$. The beam is divided into N equal intervals (N "electrons") in a phase period of 2π at the beginning of the tube, $m = 0$, and these electrons are numbered from 1 to N. A superscript i will denote the electrons as originally numbered, and a superscript j will denote a running index in

terms for a particular i.

$$\Delta\phi = \frac{2\pi}{N} \; ; \quad \phi_o^i = \frac{2\pi i}{N} \tag{III.2}$$

Y_m^{ij}, Z_m^{ij}, and F_m^{ij} are the values of the functions Y, Z, and F computed when electron i is located at m and electron j is located at its corresponding position.

The integration rule used in determining A and θ is

$$A_{m+1} = A_{m-1} + 2h \left.\frac{dA}{ds}\right|_m \tag{III.3}$$

$$\theta_{m+1} = \theta_{m-1} + 2h \left.\frac{d\theta}{ds}\right|_m . \tag{III.4}$$

The lowest-order term neglected in equation III.3 is $+\frac{1}{3} h^3 \left.\frac{d^3A}{ds^3}\right|_{m-1}$ and similarly for equation III.4. The integration rule used in determining r and ϕ is

$$r_{m+1} = r_m + \frac{h}{2}\left(\left.\frac{dr}{ds}\right|_m + \left.\frac{dr}{ds}\right|_{m+1}\right) \tag{III.5}$$

$$\phi_{m+1} = \phi_m + \frac{h}{2}\left(\left.\frac{d\phi}{ds}\right|_m + \left.\frac{d\phi}{ds}\right|_{m+1}\right). \tag{III.6}$$

The lowest-order term neglected in equation III.5 is $-\frac{1}{12} h^3 \left.\frac{d^3r}{ds^3}\right|_m$ and similarly for equation III.6. The integration rule used in forming

$$\int_{\phi_o' - \pi}^{\phi_o' + \pi} Y \, d\phi_o' \; , \quad \int_{\phi_o' - \pi}^{\phi_o' + \pi} Z \, d\phi_o' \; , \text{ and } \int_{\phi_o' - \pi}^{\phi_o' + \pi} F \, d\phi_o'$$

is simply the rectangle rule. For example,

$$\left[\int_{\phi'_o - \pi}^{\phi'_o + \pi} Y \, d\phi'_o\right]_m^i = \frac{2\pi}{N} \sum_j Y_m^{ij} . \qquad \text{(III. 7)}$$

The j's are selected to include all electrons with phases ϕ_m^j in the range $\phi_m^i \pm \pi$. Since Dq is small compared with unity, all the electrons are traveling with nearly the same velocity; hence this range in ϕ is almost equivalent to including electrons within a fixed distance on either side of electron i. The trapezoidal rule was not used for these integrals because it results essentially in a correction on the end terms of the summation, and the integrals have already been chopped off at the ends in a rather arbitrary fashion. The integration rule used in forming

$$\int_0^{2\pi} \int_{\phi'_o - \pi}^{\phi'_o + \pi} F \, d\phi'_o \sin\phi \, d\phi; \quad \int_0^{2\pi} \int_{\phi'_o - \pi}^{\phi'_o + \pi} F \, d\phi'_o \cos\phi' d\phi' \qquad \text{(III. 8)}$$

is the trapezoidal rule. As soon as there is any bunching of electrons, the ϕ_m^i's are not equally spaced in phase and, since we have computed $\int_{\phi'_o - \pi}^{\phi'_o + \pi} F \, d\phi'_o$ for the particular ϕ's, ϕ_m^i, the increments in the preceding integrals are not equally spaced. Actually, it would be possible to compute $\int_{\phi'_o - \pi}^{\phi'_o + \pi} F \, d\phi'_o$ for equally spaced phase intervals, but numerically it is much easier to compute it for the same ϕ's necessary for the space-charge terms Y and Z because all the individual terms necessary to make up F have already been calculated in that case. The term $\int_{\phi'_o - \pi}^{\phi'_o - \pi} F \, d\phi'_o$ is periodic in phase so that by using the trapezoidal rule for unequal increments equation III. 8 can be written

$$\int_0^{2\pi} \int_{\phi'_o - \pi}^{\phi'_o + \pi} F \, d\phi'_o \sin\phi' d\phi' = \frac{2\pi}{N} \left\{ \sum_{i=2}^{N-1} \left(\frac{\phi_m^{i+1} - \phi_m^{i-1}}{2} \right) \sin\phi_m^i \sum_j F_m^{ij} \right.$$

$$+ \left(\frac{\phi_m^1 - \phi_m^{N-1} + 2\pi}{2} \right) \sin\phi_m^N \sum_j F_m^{Nj}$$

$$\left. + \left(\frac{\phi_m^2 - \phi_m^N + 2\pi}{2} \right) \sin\phi_m^1 \sum_j F_m^{1j} \right\} . \quad \text{(III. 9)}$$

The small-D, thin-beam equations can now be written in finite difference form. The equations of motion become

$$p_{m+1}^i = \frac{A_m}{a} \sinh \frac{\beta_e d}{2} (r_m^i + 1) \sin\phi_m^i - \frac{\pi S}{N\beta_e d} \sum_j Z_m^{ij} \quad \text{(III. 10)}$$

$$q_{m+1}^i = \frac{A_m}{a} \cosh \frac{\beta_e d}{2} (r_m^i + 1) \cos\phi_m^i + \frac{\pi S}{N\beta_e d} \sum_j Y_m^{ij} \quad \text{(III. 11)}$$

$$r_{m+1}^i = r_m^i + \frac{\pi h}{\beta_e d} (p_{m+1}^i + p_m^i) \quad \text{(III. 12)}$$

$$\phi_{m+1}^i = \phi_m^i + \theta_m - \theta_{m+1} + h(q_{m+1}^i + q_m^i), \quad \text{(III. 13)}$$

and the circuit equations become

$$A_{m+1} = A_{m-1} \mp \frac{h}{4N\beta_e d \bar{\phi}^2 \sinh \beta_e d} \left\{ \sum_{i=2}^{N-1} (\phi_m^{i+1} - \phi_m^{i-1}) \sin\phi_m^i \sum_j F_m^{ij} \right.$$

$$\left. + (\phi_m^1 - \phi_m^{N-1} + 2\pi) \sin\phi_m^N \sum_j F_m^{Nj} + (\phi_m^2 - \phi_m^N + 2\pi) \sin\phi_m^1 \sum_j F_m^{1j} \right\} \quad \text{(III. 14)}$$

$$\theta_{m+1} = \theta_{m-1} - 2bh \pm \frac{h}{A_m 4N\beta_e d\Phi^2 \sinh\beta_e d}\left\{\sum_{i=2}^{N-1}(\phi_m^{i+1} - \phi_m^{i-1})\cos\phi_m^i \sum_j F_{rm}^{ij}\right.$$

$$\left. + (\phi_m^1 - \phi_m^{N-1} + 2\pi)\cos\phi_m^N \sum_j F_m^{Nj} + (\phi_m^2 - \phi_m^N + 2\pi)\cos\phi_m^1 \sum_j F_m^{1j}\right\} . \quad \text{(III. 15)}$$

The functions F, Y, and Z can be written

$$F_m^{ij} = \frac{\cos t_m^{ij}}{\cosh s_m^{ij} - \sin t_m^{ij}} \quad \text{(III. 16)}$$

$$Y_m^{ij} = \frac{\left[\cosh s_m^{ij} - \sin t_m^{ij} \sin r_m^i\right] \sin r_m^i \cos t_m^{ij} - \sin t_m^{ij} \cos t_m^{ij} \cos^2 r_m^i}{\left[\cosh s_m^{ij} - \sin t_m^{ij} \sin r_m^i\right]^2 - \left[\cos t_m^{ij} \cos r_m^i\right]^2} \quad \text{(III. 17)}$$

$$Z_m^{ij} = \frac{\cos t_m^{ij} \cos r_m^i \sinh s_m^{ij}}{\left[\cosh s_m^{ij} - \sin t_m^{ij} \sin r_m^i\right]^2 - \left[\cos t_m^{ij} \cos r_m^i\right]^2} \quad \text{(III. 18)}$$

where

$$t_m^{ij} = r_m^j \quad \text{(III. 19)}$$

and

$$s_m^{ij} = \frac{\pi}{\beta_e d}\left(\phi_m^j - \phi_m^i\right) . \quad \text{(III. 20)}$$

t_m^{ij} is the predicted r position of electron j when electron i is at m, and s_m^{ij} is the predicted value of the difference between the s positions of electrons i and j when i is at m. These quantities will be treated in

more detail in the discussion of the procedure for solving the equations.

3.2 Procedure for Solution

The general procedure for solving the system equations is as follows. Assume that at m = 0 the beam is unmodulated and that the amplitude A and the phase θ_o associated with the wave on the circuit are known. Now allow sufficient time so that the voltage goes through a period of 2π in phase and compute the acceleration of the N equivalent electrons uniformly distributed in phase representing the electron beams. The electron numbered N + 1 will experience the same acceleration as the electron numbered 1 so that it is only necessary to consider the N electrons distributed over a period 2π in phase. With this knowledge of the accelerations of the electrons it is possible to find the time it takes for the individual electrons to reach the next plane in s (or z), m = 1, and to find the r positions of these electrons. Since each of these electrons is accelerated in a different manner, they will not arrive at m = 1 at the equally spaced intervals in time (or phase) with which they arrived at m = 0. In addition, the presence of the beam causes the phase velocity of the circuit wave to vary as a function of m; hence the absolute time of arrival of a particular electron at m = 1 is of no immediate value. The quantity that must be known in order to compute the acceleration of the electrons at m = 1 is the phase of the voltage wave ϕ_1^i that the electrons see at m = 1. From this and the new voltage amplitude at m = 1, the time necessary to get to m = 2 can be computed. As far as the electrons are concerned, the information that is being obtained is the time at which each electron of a representative set is at

a given m position and the velocities and the r positions of these electrons when they have arrived at that position. The time is obtained in terms of the phase of the voltage wave as seen by the electrons rather than in terms of the actual time, since it is the phase that is important to the motion of the electrons.

Nothing was said about the space-charge force terms in the preceding discussion. It is clear, however, that since the position of the electrons is known only up to the plane at which the force is being computed, it is impossible to compute the space-charge forces exactly. In order to compute the space-charge force on electron i when it is at a particular position m, it would be necessary to know the position of all other electrons at that time. The procedure that is used to obtain these positions approximately is linear extrapolation. The velocity of all the electrons is known for a particular m, and the times that these electrons are at this plane are also known. It is assumed that the electrons continue to travel at the same velocity after they leave this particular plane so that their position as a function of time can be computed. Using the definition of ϕ, equation II.36, the difference in time between the arrival of electron i and that of electron j at position m is

$$t^j_m - t^i_m = \frac{1}{\omega}\left(\phi^i_m - \phi^j_m\right) . \qquad \text{(III.21)}$$

Electron j is traveling with z velocity

$$\frac{dz^j}{dt} = u_o\left[1 + 2Dq^j_m\right] \approx u_o \qquad \text{(III.22)}$$

and y velocity

$$\frac{dy^j}{dt} = 2u_o Dp^j_m \approx 0 \ , \qquad \text{(III.23)}$$

so that to a first approximation electron j is located at r^j_m and a distance

$$z^j - z^i_m = \frac{u_o}{\omega}\left(\phi^j_m - \phi^i_m\right)$$

away from electron i, when i is at m. t^{ij}_m and s^{ij}_m can now be written

$$t^{ij}_m = r^j_m$$

and

$$s^{ij}_m = \frac{\pi}{\beta_e d}\left[\phi^j_m - \phi^i_m\right] .$$

With this information it is now possible to compute F^{ij}_m, Y^{ij}_m and Z^{ij}_m from equations III.16, III.17, and III.18. It is possible to make this simple approximation for the electron positions because, for typical values of $\beta_e d$, the functions F, Y, and Z are rapidly decreasing functions of $z^j - z^i$ so that as the approximation becomes worse, the relative effects of these electrons become less. In the numerical work, only electrons within a phase $\pm \pi$ of the particular electron in question are used in computing the force on that electron. Another difficulty encountered in computing the space-charge forces is that introduced by replacing a cylindrical volume of charge by an equivalent line charge. The force between two line charges goes to infinity as the charges approach each other so that some assumption must be made about the short-range forces. These are assumed to be zero within a radius ϵ of the line charge. The radius ϵ is chosen from numerical considerations and a correction factor

must be applied to the space-charge parameter to account for the fields eliminated. This point is discussed further in Chapter IV in comparing the computional results with previous small-signal results.

The effect of the beam on the circuit wave is computed in the following manner. The actual flux terminating on the circuit at m due to all the charges is computed at the time that each different electron is at m so that when this procedure has been completed a graph of E_{ym} at the circuit as a funtion of time (or phase) can be plotted. The second time derivative is taken to obtain the time rate of change of displacement current, which is the driving term in the circuit equation, and this is Fourier analyzed to obtain the fundamental component in accordance with the assumptions concerning the circuit.

The actual procedure for solution of the equations may be summarized as follows:

1. A_m, θ_m, p^i_m, q^i_m, r^i_m, and ϕ^i_m are known at m = 0 for i = 1, 2, 3, . . . , N.
2. Select a particular electron i and another electron j and compute t^{ij}_m and s^{ij}_m from equations III.19 and III.20, and F^{ij}_m, Y^{ij}_m, and Z^{ij}_m from equations III.16, III.17, and III.18.
3. Repeat this procedure for the N different j's that have $\left|\phi^i_m - \phi^j_m\right| \leq \pi$. This means that, at times, j corresponds to an electron outside of the range 1 to N, but since $\phi^{j+N}_m = \phi^j_m + 2\pi$, there is no complication.
4. Form the $\sum_j Y^{ij}_m$, $\sum_j Z^{ij}_m$, and $\sum_j F^{ij}_m$. Use equations III.11, III.12, III.13, and III.14 to compute p^i_{m+1}, q^i_{m+1}, r^i_{m+1}, and ϕ^i_{m+1}; store $\sum_j F^{ij}_m$ for use in computing A_{m+1} and θ_{m+1}.

5. Repeat steps (2), (3), and (4) for i = 1, 2, 3, ...N.

6. Use the values of $\sum_j F_m^{ij}$ obtained in step (4) to compute A_{m+1} and θ_{m+1}. All of the quantities in step (1) are now known at m + 1, and the cycle can be repeated to advance to m + 2, etc.

The oscillation conditions for a backward-wave oscillator[12] [13] are determined by assuming a value of A_o, the amplitude function, and b, the velocity difference parameter, and integrating the equations. If A decreases to zero at some point along the tube, the gain in the backward direction will be infinite and the tube will oscillate. Only one value of b will cause the amplitude to go to zero for any particular value of A_o. The velocity parameter actually determines the oscillation frequency for a particular circuit since b and u_o determine v_o, the circuit phase velocity, and for a dispersive circuit v_o determines a particular frequency. The point at which the amplitude goes to zero determines the starting length of the tube as an oscillator. Experimentally, the tube is generally of fixed length and the current is varied. Since the normalized z coordinate is proportional to $\sqrt{I_o}$, a different value of starting length can be regarded as a change in the tube current, and the different values of b associated with different values of A_o actually determine the frequency pushing with tube current.[13]

The forward-wave-amplifier cases are carried out by assuming a value of A_o and a value of b and integrating the equations until most of the electrons are collected on the circuit or the amplitude function begins to decrease because the electrons have gone into the wrong phase.

In this case the frequency is regarded as fixed, and the value of the velocity parameter b determines how far from synchronism the beam velocity and circuit-wave velocity are.

3.3 Errors and Computing Time

The problem of numerical errors in the computations was attacked from an experimental point of view. The errors considered here are errors only with respect to the accuracy of solution of the integral-differential equations describing the system and not with respect to the accuracy with which these equations describe the physical situation. The choice of the integration interval h, the number of electrons N, and the computation time resulting for a particular choice of h and N are discussed. The selection of h and N was made by computing the same cases for different values of h and different values of N. From the standpoint of accuracy, one would like to choose a value of h small enough and a value of N large enough so that making h smaller or N larger would have no effect on the solution. However, to minimize the computing time one would like to choose h as large as possible and N as small as possible since the computational time is inversly proportional to h and approximately proportional to N^2.

Two sample cases were calculated for various values of h. With the space-charge parameter S equal to zero, there is virtually no difference between solutions for h = 1/32 and h = 1/64 and only a slight difference between solutions for h = 1/16 and h = 1/32. The value h = 1/16 changed the starting length for a small-signal, backward-wave-oscillator case by about 1 part in 100 over the value for h = 1/32. The

value h = 1/16 would be suitable for S = 0. With the space-charge parameter S = 3, a set of solutions was run for h = 1/16, 1/32, 1/64, 1/128, and 1/256. The amplitude function still differed by about 1 part in 20 at the end of the tube for the two cases h = 1/128 and h = 1/256. The solutions appeared to be converging, however, and there was no difference in the nature of the results; hence a value of h = 1/64 was finally chosen for all computations. Since the equation for θ has a factor A in the denominator, in the backward-wave-oscillator cases where the circuit amplitude A is approaching zero $\frac{d\theta}{ds}$ is very large and an error in A that is small in magnitude can produce an error in θ that is large in magnitude. The error in A is relatively insignificant, but the error in θ means that the electrons are shifted into the wrong phase and this significantly affects the solution. Fortunately, this occurs over only a relatively short region as A approaches zero; although it is difficult to obtain the start-oscillation conditions precisely, there is no difficulty in determining a range within which these conditions must lie that will determine the starting length within about five percent. A value of N = 33 was selected primarily on the basis of minimizing computing time. A larger value of N would be desirable, particularly for those cases in which the space-charge parameter is large. The nature of the results is not affected when N is changed from 33 to 67, and it was felt that the gain in accuracy does not justify the large increase in computing time. If the space-charge parameter is zero, there is only a slight difference in the results for cases in which N = 16 and N = 33. In the large-signal analysis of the ordinary traveling-wave tube a value of N = 24 was found

to be satisfactory for most cases, although a larger value of N becomes necessary as the space-charge parameter is increased to correspond to very high current density beams.[9] [10]

The computing time per integration m for N = 33 on IBM 704 equipment is about 20 seconds. Since the starting lengths for the backward-wave-oscillator cases are in the neighborhood of s = 1.5, a complete case requires about 30 minutes. The computing time is approximately proportional to N^2 because for each individual electron the space-charge terms must be computed for all other electrons. Therefore, the space-charge terms must be computed N^2 times per integration step. Because Y, Z, and F are quite complicated functions, a major part of the computational time is devoted to computing the space-charge functions.

IV. COMPARISON OF RESULTS WITH PREVIOUS WORK

During the course of checking out the computer program, a number of small-signal, backward-wave-oscillator cases were computed for comparison with previous theoretical results. The agreement with these results is good and creates confidence in the large-signal calculations. Some difficulties were experienced in the space-charge cases because of the nature of the short-range force between line charges that was assumed initially. A "breakup" of the beam similar to that reported in hollow electron beams[15] developed very rapidly and masked the circuit interaction effects. By modifying the force law at short ranges so as to reduce the force between two elements of charge, it was possible to substantially eliminate the beam breakup. It was then necessary to introduce a space-charge correction factor to bring these results into agreement with the small-signal analytical results.

Numerical calculations are compared with previous work in three different situations. In the first section, results for small-signal and no space charge are compared with previous work for a variety of the parameters that must be specified in the numerical calculations. In the next section, results for small signals, including space charge, are compared with previous work and a space-charge correction factor is introduced. In the last section, some large-signal, no space-charge cases are compared in a qualitative fashion with the work of Feinstein and Kino.

4.1 Small-Signal, No Space-Charge Results

The start-oscillation conditions for a thin-beam, crossed-field, backward-wave oscillator under small-signal conditions, neglecting

space-charge effects, have been determined analytically by Muller[3] using the theory of Pierce.[2] The result is that the amplitude of the circuit wave varies as $\cos \beta_e Dz$ (or $\cos s$), so that the length of tube required to start oscillation is $s = \pi/2$. The velocity difference parameter b is zero for this case; the circuit wave and the beam are in exact synchronism. In this type of small-signal analysis it is assumed that the beam moves only very slightly from its equilibrium position so that the ratio $E_y/E_z = a$ does not change and the beam position can be specified in terms of a alone. In the analysis presented here, it was anticipated that, under large-signal conditions, the beam would change its position and that therefore the ratio of the fields acting on the beam would change, depending on its actual location. The position of the beam and the circuit-to-sole spacing must be specified; these quantities determine a. The starting lengths of a backward-wave oscillator as computed from the equations presented here are given in Table 1 for several values of the circuit-to-sole spacing in electronic wavelengths, $\beta_e d$. The velocity difference parameter b is zero in all cases.

Table 1. The computed starting length of a crossed-field, backward-wave oscillator with space-charge effects neglected. The small-signal analytical result is $s = \pi/2 \cong 1.57$.

$\beta_e d$	r_o	(b)start	(s)start
2.0	0	0	1.57
2.0	-0.25π	0	1.56
2.5	-0.30π	0	1.54
3.0	-0.33π	0	1.50
3.5	-0.36π	0	1.44

The first two cases shown in the Table are for $\beta_e d = 2$ and for the beam one-half of the way from the sole to the circuit and one-fourth of the way from the sole to the circuit, respectively. The first case checks the analytical result very accurately and the second case is very close, but s is a little small. The next three cases are for $\beta_e d = 2.5$, 3, and 3.5, with the beam injected relatively close to the sole in each case; the calculated starting length becomes progressively shorter as $\beta_e d$ is increased. The small-signal analytical result is $s = \pi/2$ and $b = 0$ for all cases. The increased error for large $\beta_e d$ is due to the neglect of electrons beyond $\pm \pi$ of the phase for which the field terminating on the circuit is being computed.

Consider a beam perturbed as illustrated in Fig. 8a; the pattern can be regarded as sliding towards the right and we will consider the phase at z to be $\phi = \pi/2$. The charge that is included in computing the flux terminating on the circuit at z at $\phi = \pi/2$ is that charge contained between the short vertical lines at $\phi = -\pi/2$ and $3\pi/2$. In Fig. 8b, the field terminating on the circuit at z, $E_{sy}(\frac{d}{2}, z)$, is plotted as a function of the phase at z. The horizontal dashed line is a line of constant E_{sy} as a function of phase that would result if the beam were unperturbed. If all the charge were included, a curve of E_{sy} versus ϕ might appear as the one marked exact computation, and if only charge within a phase $\pm\pi$ were included, the curve might appear similar to the one marked approximate calculation in Fig. 8b. This can be demonstrated by considering two phases, $\phi = \pi/2$ as indicated in Fig. 8a and another case in which the phase is π later so that the beam shape in Fig. 8a has slipped to the

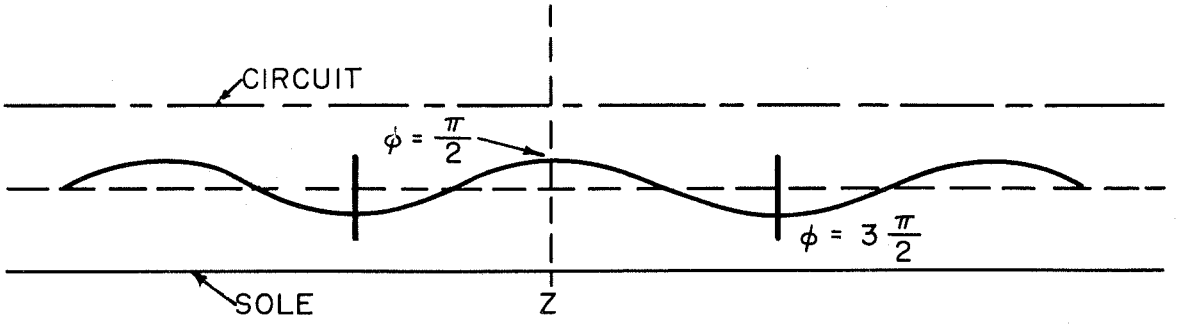

Fig. 8a. The perturbed electron beam

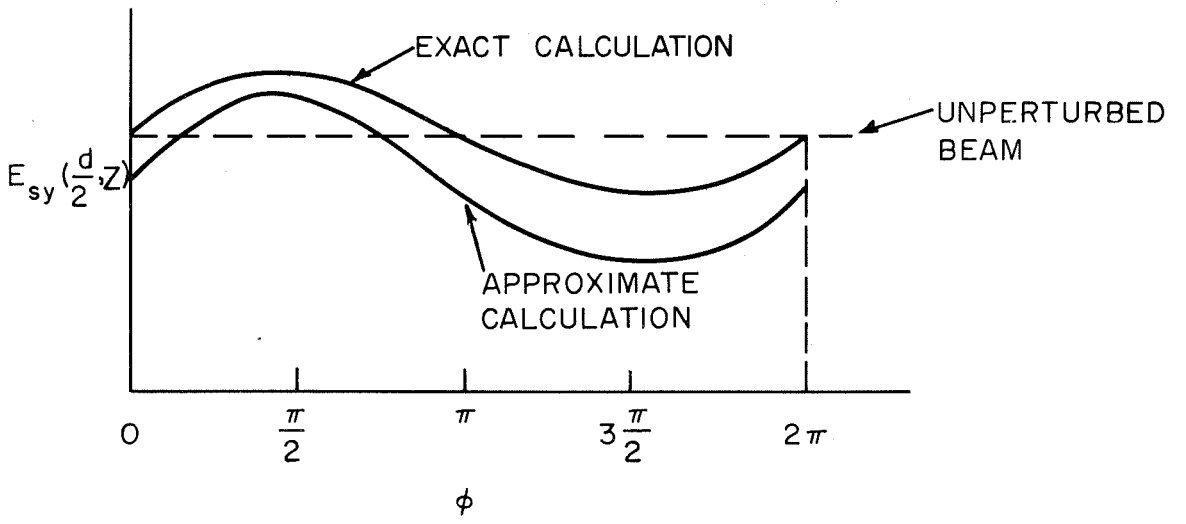

Fig. 8b. The fields terminating on the circuit at Z as a function of phase (or time)

right until $\phi = -\pi/2$ is at z. The total charge included is always less in the approximate calculations than in the exact calculations so that the field terminating on the circuit will be smaller for all phases in the approximate calculations. For $\phi = \pi/2$ the charge nearest to z that is excluded is the charge at $\phi = -\pi/2$ or $3\pi/2$, which is further away from the circuit in the y direction than the average, whereas for $\phi = -\pi/2$ (or $3\pi/2$) the nearest charge excluded is that at $\phi = \pi/2$ or $-3\pi/2$, which is closer to the circuit than the average so that, in effect, more field has been neglected at $-\pi/2$ (or $3\pi/2$) than at $\pi/2$, and the curve of E_{sy}, instead of being simply displaced downward, is displaced downward more at $3\pi/2$ than at $\pi/2$. The alternating component of E_{sy} is therefore larger in the approximate case than in the exact case and, since this is the driving term in the circuit equation, the beam modulation appears to be larger than it actually is and the starting length is shorter. For larger $\beta_e d$ the fields from a given charge effectively extend further in the z direction and the terms neglected become larger.

The errors described above could be reduced by including charge further from the point of interest if necessary. To compute the fields for these added electrons by means of the space-charge functions F, Y, and Z would increase the computing time proportionally to the square of the number of electrons included. It was decided to carry out the calculations for $\beta_e d = 2.5$ and the beam one-fifth of the way from the sole toward the circuit. This is a fairly representative value of $\beta_e d$; magnetrons are normally designed with βd equal to 3, and backward-wave amplifiers are generally designed to operate between $\beta d = 2$ and $\beta d = 3$.

For this value of $\beta_e d$ the error in starting length is only about 1 part in 50 and no additional charge was included in the calculations.

4.2 Small-Signal, Space-Charge Results; A Space-Charge Correction Factor

The problem of a beam in crossed electric and magnetic fields interacting with a slow-wave circuit under small-signal conditions and including space-charge interaction effects has been attacked most successfully by Gould.[5][6] The comparison made here is with the second paper by Gould, which is concerned with the case in which the beam can be considered to be thin. The results presented here are in one sense a comparison and in another sense a justification of the procedure used in calculating the space-charge effects. One of the difficulties encountered in replacing a volume element of charge by a line charge is that such replacement introduces an infinity in the electric field at the charge. In order to remove this infinity, it is necessary to make some assumption about the behavior of field in the vicinity of the line charge. The fields are assumed to be zero in the immediate vicinity of the charge. The calculated forces are therefore less than would be obtained if the exact fields were used, and a correction must be applied to the space-charge parameter. The agreement between the results obtained here and the analytical work by Gould is relatively good when this correction factor is included.

The first assumption made regarding the field in the vicinity of a line charge was based on the fact that, within a circular cylinder of charge, the electric field increases linearly from zero at the center to

a maximum at the edge, a maximum which is exactly equal to the field of a line charge located at the center and having a charge equal to the total charge in the cylinder. In early computations it was assumed that the field increased linearly from zero at the charge to the value given by the functions Y and Z at some arbitrary distance ϵ away from the charge, as illustrated in Fig. 9. The distance ϵ was chosen to be of the order of the separation between line charges in the unperturbed beam. Computations carried out with this short-range force law were not very successful; computer errors built up and masked the interaction effects. Some electron phase diagrams for typical cases are shown in Figs. 10 and 11. These diagrams show the transverse position of the electrons as a function of phase after the electrons have traveled a distance along the tube. The points have not been marked on these curves, but they are connected by straight lines. Since the electron drift velocity is always very nearly u_o, these diagrams are approximate pictures of the beam shape at various positions along the tube. Figs. 10 and 11 are drawn for the same tube parameters but were computed by using 33 and 67 electrons, respectively; the scale in r is the same for both figures. The total displacement of the beam from equilibrium is very small so that these cases truly correspond to small-signal calculations and the actual numerical value of r is not significant. The distance ϵ was chosen to be exactly the separation between line charges in the unperturbed beam in each case so ϵ in Fig. 11 is one-half of ϵ in Fig. 10. The errors build up faster for 67 electrons than for 33 electrons; the curve for N = 33 is at

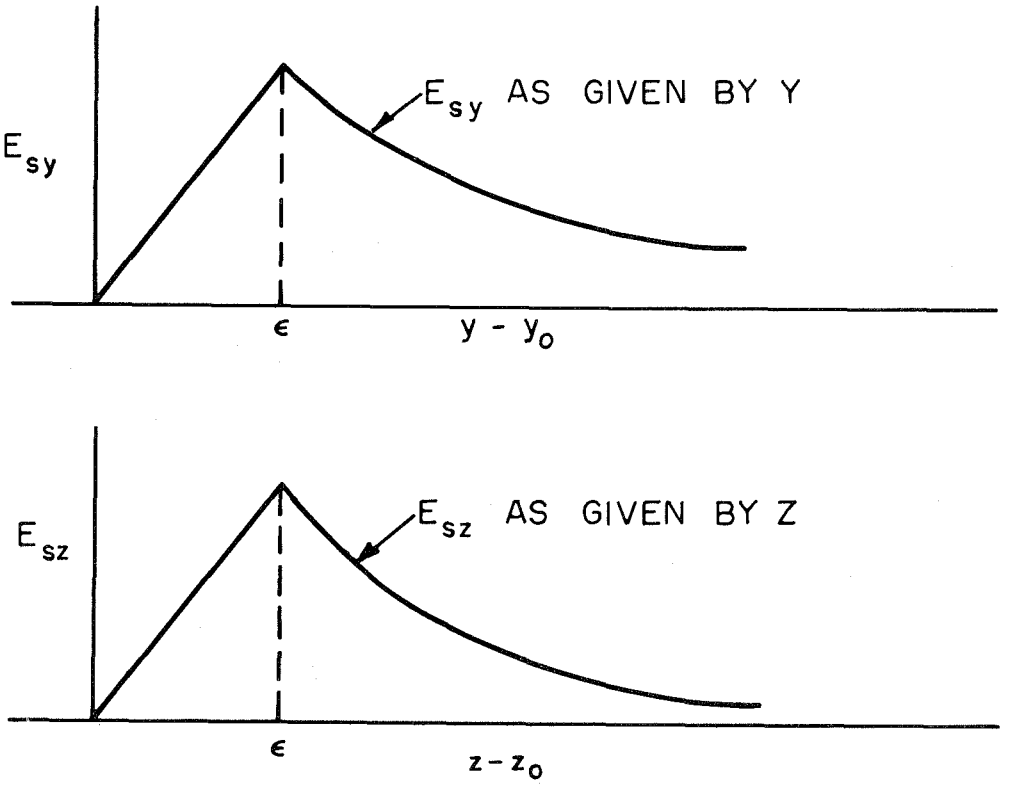

Fig. 9. The initial assumption regarding the fields in the vicinity of a line charge

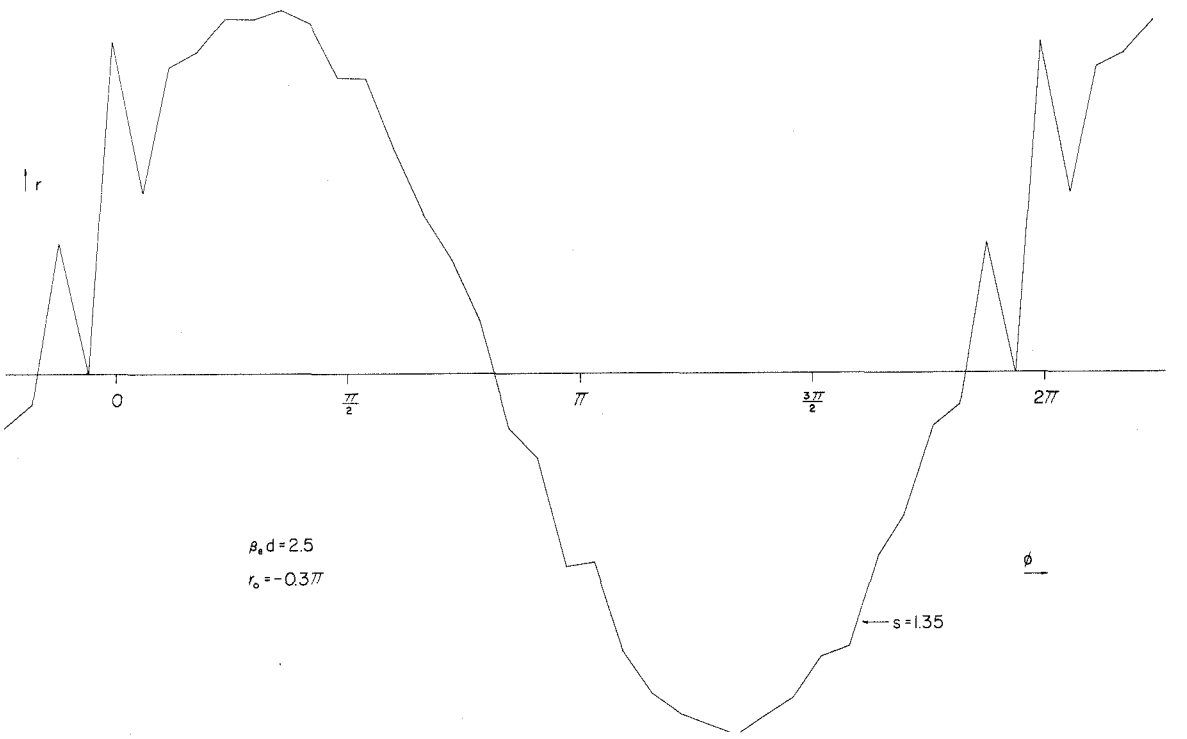

Fig. 10. Breakup of a thin beam, 33 "electrons"

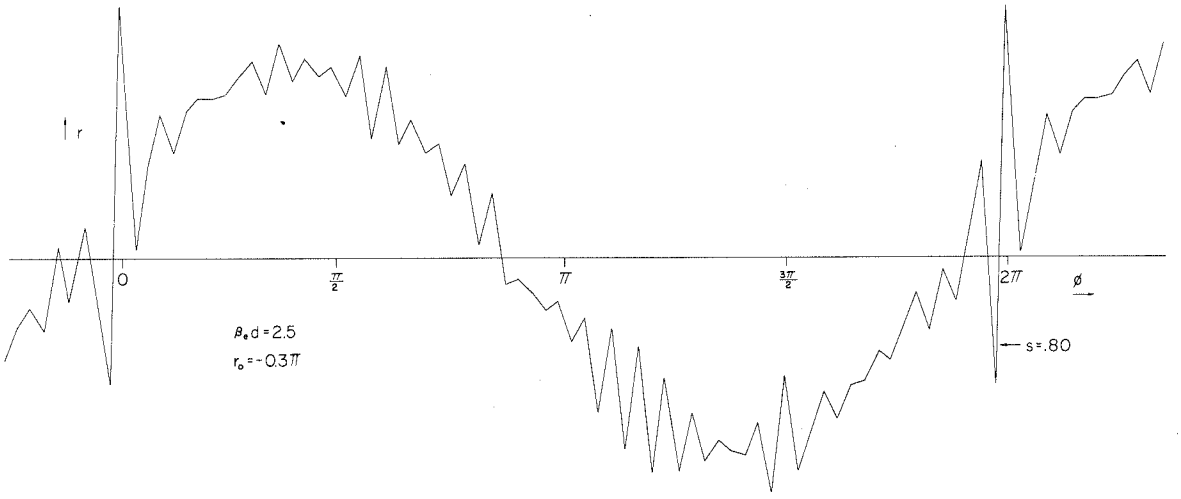

Fig. 11. Breakup of a thin beam, 67 "electrons"

s = 1.35 whereas the curve for N = 67 is only at s = 0.8 and the perturbations are already larger for N = 67 than for N = 33. The jagged appearance of the electron beam which develops as the beam progresses down the tube is a result of the discrete nature of the numerical solutions. Adjacent line charges produce very strong forces on each other that are nearly balanced by the other charges. A slight error in the location of one of these charges results in a force which is not properly counterbalanced by the other charges and the charge is forced further out of position and causes unbalanced forces on the neighboring charges. The process grows very rapidly until it predominates over the original motion. Going to a smaller integration interval does not alleviate the difficulty, which would indicate that the errors are in the subroutines and not in the integration techniques. Increasing the value of ϵ improves the situation only very gradually.

The breakup of the smooth beam shape described above is a short-wavelength manifestation of the growth of space-charge waves on a beam of electrons in crossed electric and magnetic fields (termed the diocotron effect by the French). It is also closely related to a situation observed experimentally in thin, hollow, cylindrical beams of electrons[15] and treated theoretically by several workers[16][17]. In this case the electrons are traveling parallel to a strong magnetic field, and the cross section of the beam starts out as a thin, circular strip at the cathode and eventually breaks up into a number of filamentary beams located around the circumference of the circle. If the motion along the direction of the magnetic field is disregarded and if the radius of the beam is large, the

situation is similar to a thin beam in crossed fields viewed from a coordinate system moving with velocity $u_o = E_o/B_o$ so that the static electric field disappears. Kompfner[18] carried out some numerical calculations for this case and found that due to computer errors, the line charges would eventually tend to break up into pairs quite similarly to what happens in Figs. 10 and 11.

The solution for space-charge waves on a thin beam of electrons drifting in crossed electric and magnetic fields shows that the perturbations grow exponentially with time in a coordinate system moving with the electrons and the exponent is inversely proportional to the wave length of the disturbance so that the shortest wavelength disturbance grows faster than all others.[6] For the numerical calculations carried out here, the shortest effective wavelength is that corresponding to twice the separation between two electrons, and a disturbance in the positions of any individual pair of electrons would tend to grow much faster than the effects of the circuit interaction. The difference in the rates of growth for the circuit wavelength and the perturbations is the ratio of the effective wavelengths (33/2 for 33 electrons and 67/2 for 67 electrons). Since this factor appears in the exponent, it would be extremely difficult to reduce the computer errors so as to completely eliminate this effect.

A rather drastic assumption regarding the fields in the vicinity of a line charge was necessary to circumvent the difficulty described above. It was assumed that the fields were zero out some distance ϵ and that they then behaved exactly like the fields from a line charge

(Fig. 12). The distance ϵ was chosen to be 3/2 times the spacing between electrons so that in an unperturbed beam an electron produced no force on the immediate neighbor electron on either side. This force law successfully eliminated the error buildup described above. No difficulties were encountered for the values of S used in the calculations. One question that arises here is that since this buildup is in a sense related to an actual physical situation, should it be eliminated? The answer is that (1) the buildup in the computations is due to computational errors, not to actual perturbations on the electron beam and (2) in the case of a beam of finite thickness the rate of growth of space-charge waves does not increase monotonically with decreasing wavelength but reaches a maximum and then decreases to zero.[5] The problem as treated here may be regarded as representing a sort of equivalent thick beam.

The small-signal start-oscillation conditions were determined for $\beta_e d = 2.5$, $r_o = -0.3\pi$, and S = 0, 1.5, 3, and 4. The space-charge correction factor that will be introduced makes the effective values of S be 0, 1.1, 2.2, and 2.92. Fig. 13 is a plot of s(start)/2π, which is equal to D times the number of electronic wavelengths on the circuit, as a function of the space-charge parameter S. A similar curve taken from Reference 4 is plotted on the same graph; although the curves have the same general shape, which shows the familiar reduction in starting length with increase in space charge, there is an appreciable quantitative difference. Fig. 13 is for $\beta_e d = 2.5$ and

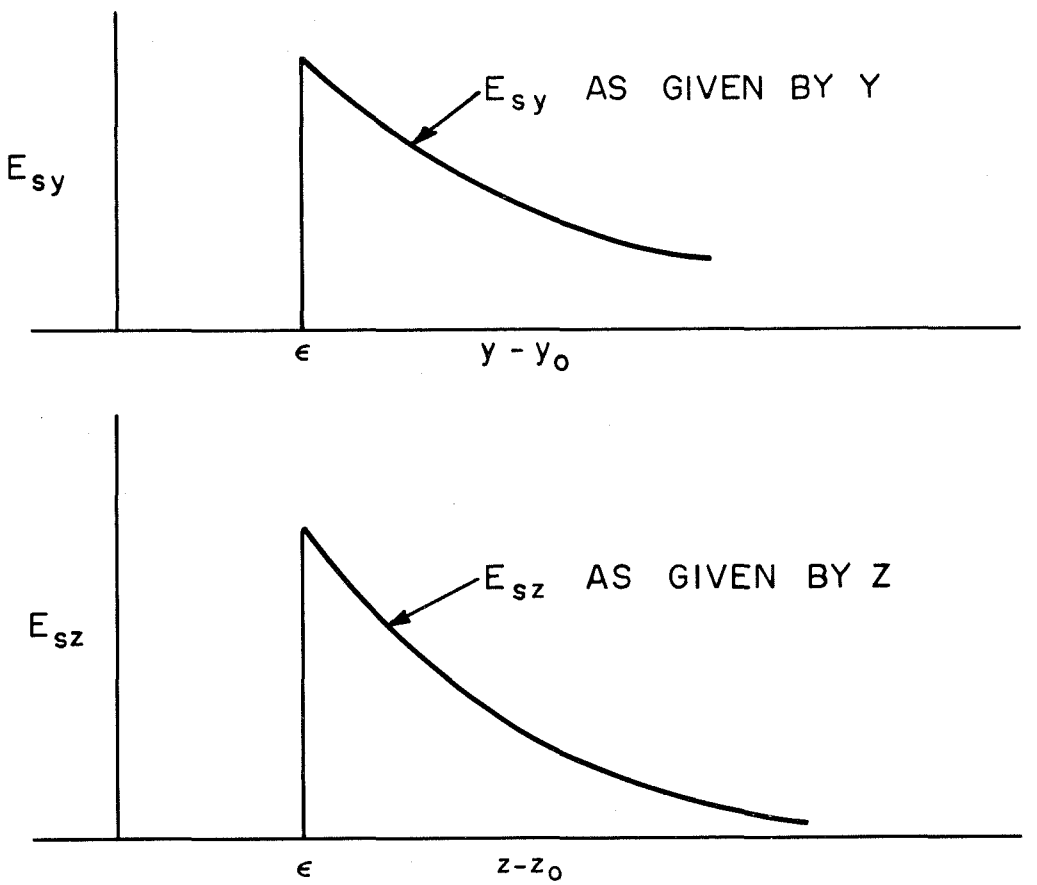

Fig. 12. The fields in the vicinity of a line charge as used in the computations

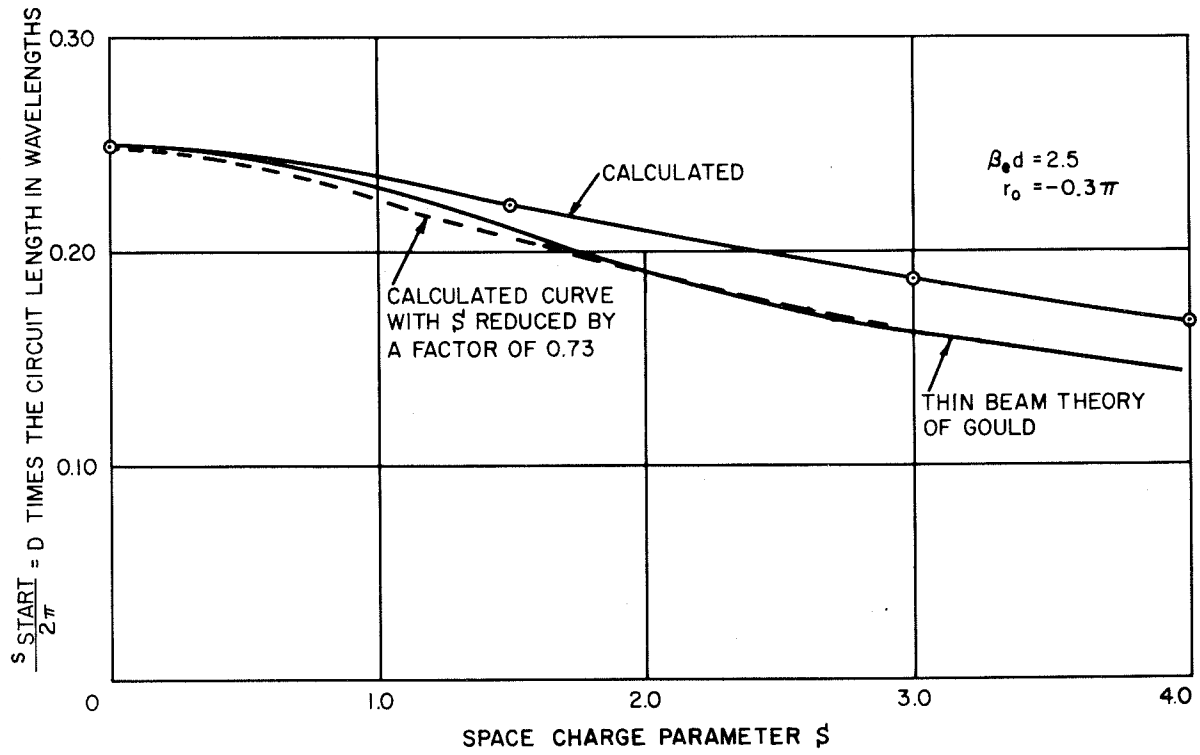

Fig. 13. The starting length of a backward-wave oscillator as a function of the space-charge parameter S

$r_o = -0.3\pi$ and Fig. 14 is a similar set of curves for $\beta_e d = 2.0$ and $r_o = 0$. The dashed curve in each of these figures is the calculated curve replotted with S reduced by a factor of 0.73, which will be regarded as a space-charge correction factor applicable to the particular computations in which 33 electrons are used and the short-range forces behave as described in Fig. 12 with ϵ chosen to be 3/2 times the separation between line charges in the unperturbed beam. The introduction of this factor is empirical and is supported by the fact that the same factor works quite well in cases which have the same geometry but different values of S and also in cases which have quite different geometries. One would certainly not expect that the nature of the results would be determined by the immediately neighboring charge; therefore it seems reasonable to introduce a correction factor to account for the neglected charge. Actually, another, better type of correction factor might be one which would weight the nearer charges more heavily than the distant charges. However, such a factor was not used because of the complications it would have introduced into the computer programming. The factor 0.73 has been applied to S in all the large-signal calculations.

Fig. 15 is a curve of the velocity injection parameter b for small-signal oscillation as a function of the space-charge parameter S. It should be emphasized that b is defined in terms of the phase velocity of a free wave on the circuit and the average drift velocity of an electron in the absence of space charge,

$$u_o = \frac{E_o}{B_o} = v_o(1 + Db) \qquad \text{(IV.1)}$$

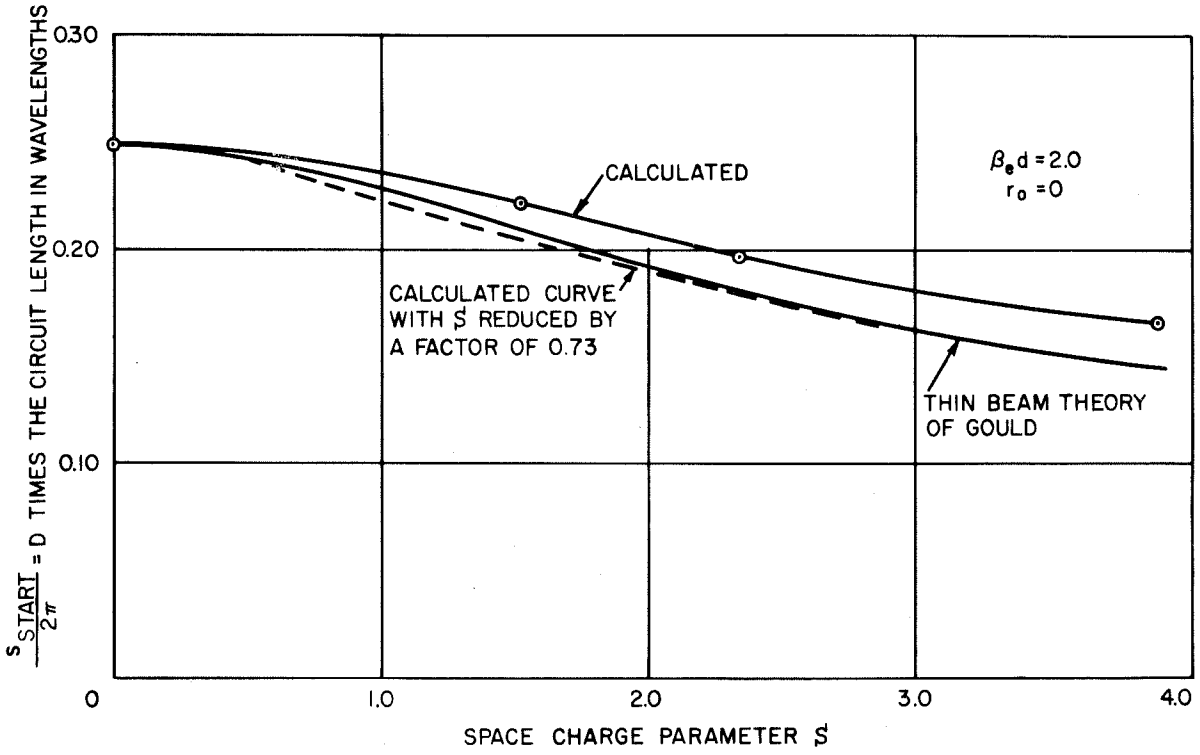

Fig. 14. The starting length of a backward-wave oscillator as a function of the space-charge parameter S

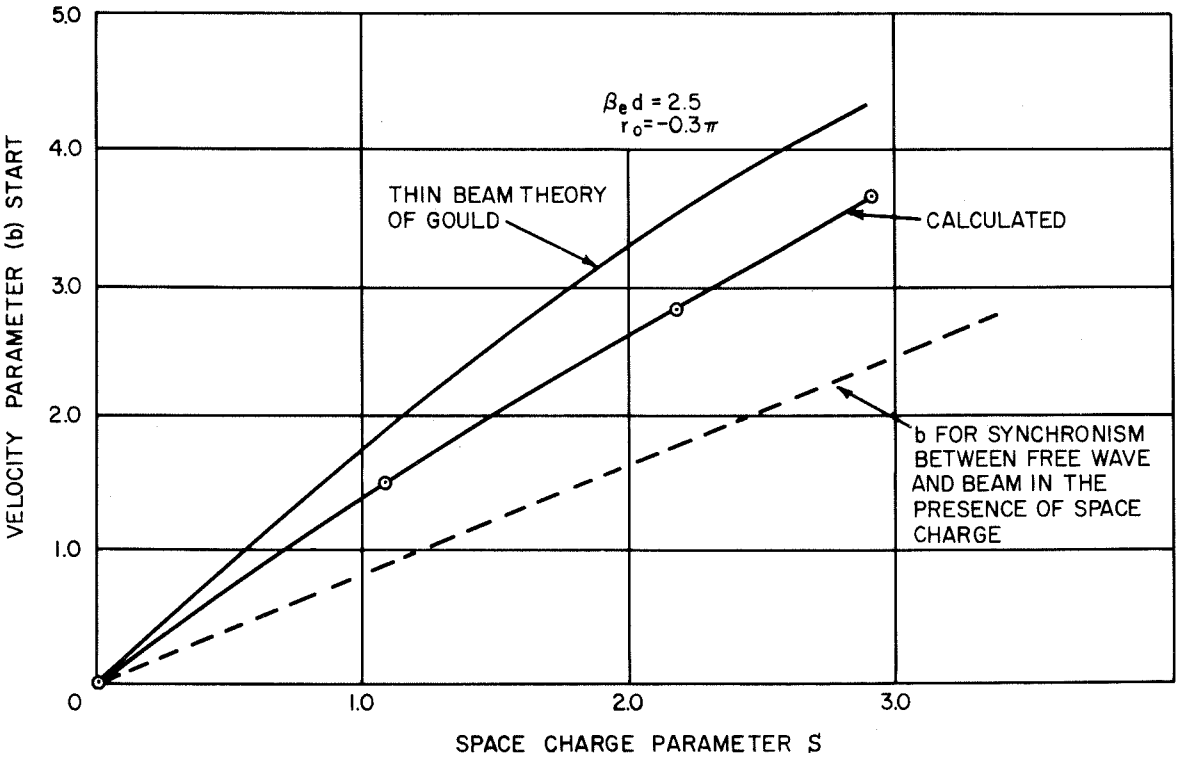

Fig. 15. Velocity-injection parameter for start oscillation versus the space-charge parameter

so that if the space-charge effects are included, there will be an average drift velocity which differs from E_o/B_o and depends on the space-charge parameter and the location of the beam with respect to the circuit. The value of b necessary to make the average drift velocity of the electrons equal to the free-wave velocity is shown as a dashed line in Fig. 15. The velocity injection parameter as obtained from the thin-beam analytical work is also plotted in Fig. 15; it is appreciably different from the value obtained here. This difference may be due to numerical errors because some calculations indicate that reducing the integration interval to a value less than 1/64 increases the value of b required for start oscillation. The data are not sufficient to show that the magnitude of the change in b is enough to account for the difference shown in Fig. 15. The reason for the error in b is that $d\theta/ds$ is inversely proportional to the circuit amplitude so that near the end of the tube, where the amplitude is approaching zero, the error in θ can become quite large, but it can be compensated for by a change in b which keeps the beam near synchronism.

As the space-charge parameter is increased, the beam must be injected at higher velocity to obtain oscillation. The interesting point to note about this effect is that the actual phase velocity of the circuit wave at oscillation is not affected by a change in the space-charge parameter. Although the electron trajectories change appreciably as the space-charge parameter is increased, the velocity of the circuit wave is still the free-wave velocity. Figs. 16 and 17 are electron phase plots for a small-signal, start-oscillation case with S = 0 and

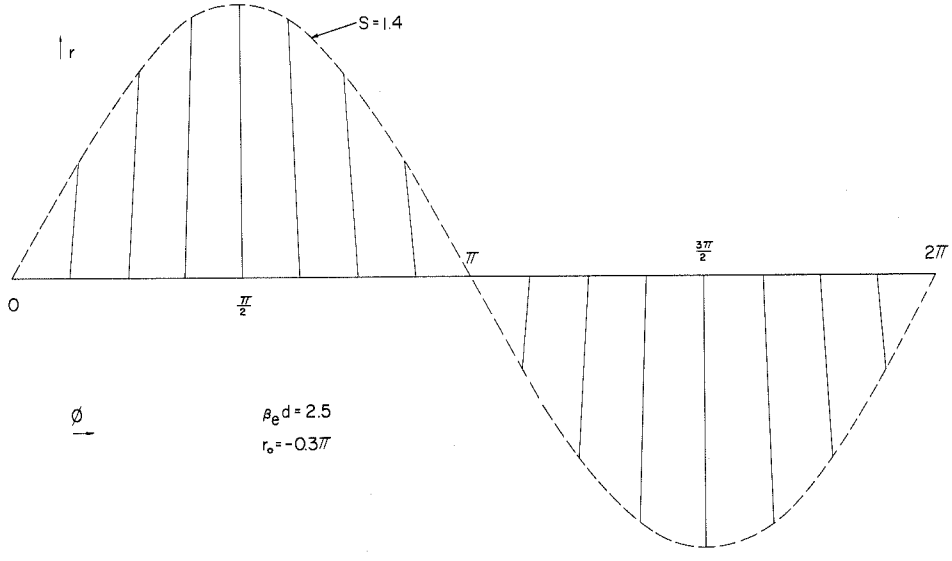

Fig. 16. Electron phase plot for start oscillation with S = 0

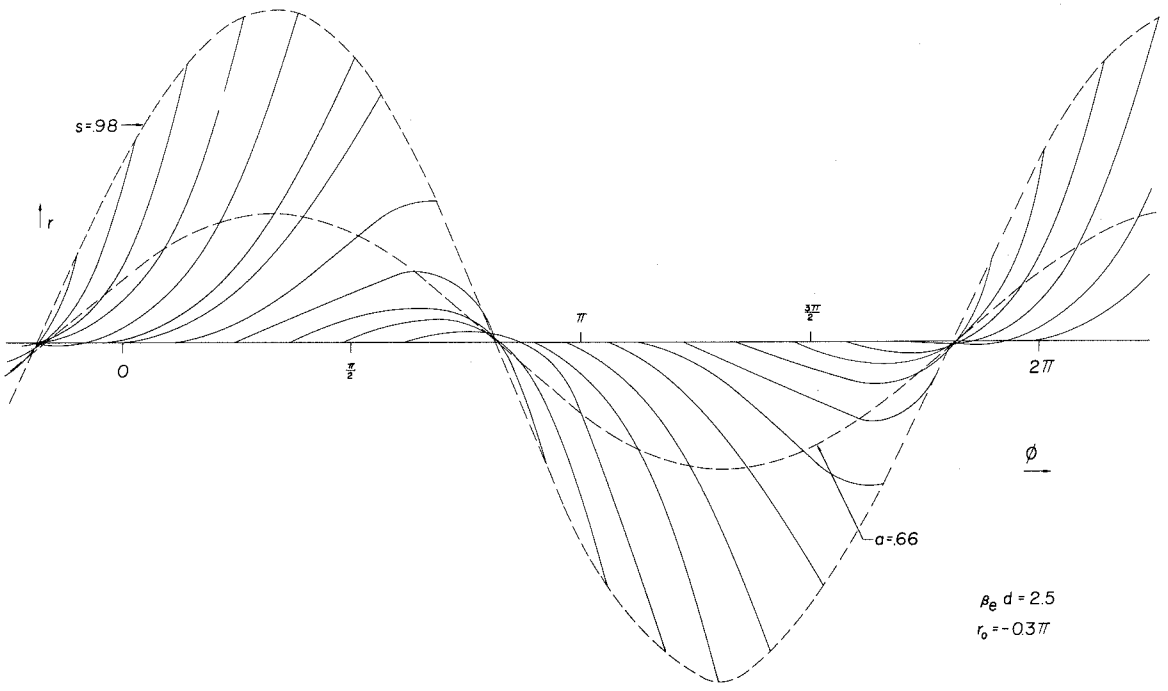

Fig. 17. Electron phase plot for start oscillation case with S = 2.92

S = 2.92, respectively; the total r deviation of the beam in each case is very small. The solid lines indicate the motion in phase of a typical set of electrons; the dashed lines indicate the beam surface at a particular position along the tube. The straight, horizontal line is the unperturbed beam surface at the beginning of the tube. In Fig. 16, the case with S = 0, the electrons tend to bunch about phase $\pi/2$ and always remain in synchronism with the wave. In the space-charge case (Fig. 17), the electrons are slipping through the wave, but they slip at just such a rate that the beam boundary always remains sinusoidal, with the maximum at nearly $\phi = \pi/2$, just as in the no space-charge case, and there is little tendency for the phase velocity of the wave to change. The electrons do not particularly tend to bunch in the space-charge case; they remain more or less uniformly distributed in phase.

The results presented here appear to agree quite well with small-signal analytical results and create a certain amount of confidence that the equations are correct and that the computer program is operating properly. The result that the circuit wave velocity does not change even when space-charge effects are present could be of use in other analytical approaches to the problem because it is quite easy to determine the rate of change of the amplitude of the circuit wave but more difficult to determine the rate of change of the phase.

4.3 Large-Signal, No Space-Charge Results

The only previous work of this sort known to the author is that of Feinstein and Kino.[4] The comparison with their work is only qualitative for the following reasons. In order to simplify their calculations

they placed the sole essentially at infinity (this makes $\left|\frac{E_y}{E_z}\right| = 1$ everywhere), but they still collected electrons on a fictitious sole at a position corresponding to $\beta_e d = 3.5$. In order to accomplish the same effect in the present computations, $\beta_e d$ would have to be equal to about 6 or larger, and the beam would then have to be introduced near the circuit and electrons collected on a fictitious sole at a distance $\beta_e d = 3.5$ away from the circuit. Unfortunately, since the value $\beta_e d = 6$ is large enough to produce a significant error in the approximations, as was noted previously, this particular case was not attempted. The artifice of using a fictitious sole actually produces results different from those that would be obtained with a conducting sole because the tangential electric field on the artificial sole is not zero. Since under the assumptions used here, electrons move perpendicular to the electric field, electrons would be collected on the artificial sole that would not ordinarily be collected when the tangential field is zero. The results with space-charge effects neglected will be described qualitatively here and presented in more detail in the next chapter, along with the other large-signal computations.

If space-charge effects are neglected, the oscillation condition, even with large signals, is that the velocity parameter b equal zero and that the phase velocity of the wave remain unchanged. This result could be anticipated from a consideration of the small-signal phase diagram presented in Fig. 16 and is one of the assumptions used by Feinstein and Kino in carrying out their analysis. Initially, the starting length of the oscillator decreases with increasing amplitude and then increases again. The reason for the initial decrease in length is that the beam is moved

nearer to the circuit into regions of higher field strength. Eventually, part of the beam is collected on the circuit before the end of the tube, and the starting length increases until the amplitude is so large that all the beam is collected before the oscillation condition has been reached. This result is similar to that obtained by Feinstein and Kino.[4]

V. LARGE-SIGNAL CALCULATIONS

The results of large-signal calculations for typical cases are presented in this section. The saturation power that is available from the system is discussed first, and an upper bound for the normalized circuit amplitude is determined for a backward-wave oscillator. Computations covering a variety of backward-wave-oscillator, backward-wave-amplifier and forward-wave-amplifier cases are then discussed.

5.1 Saturation Effects

An effect commonly observed in high-power traveling-wave tubes is that as the r-f input power is increased, the output power increases initially, eventually reaches a maximum value, and then decreases again. In the ordinary traveling-wave tube in which the beam is confined by a strong axial magnetic field so that it moves only along the axis of the tube, this saturation is a result of the fact that the electrons give energy to the wave by decreasing their kinetic energy. The electrons that are initially in a decelerating phase of the wave slow down until eventually they are moving more slowly than the circuit wave; they slip into an accelerating phase and abstract energy from the wave and the output no longer increases. If the tube is still longer, electrons continue to interact with the wave past the point of maximum amplitude, the circuit amplitude begins to decrease again and at the output it may actually be less than it is at some preceding point along the tube. For an ordinary traveling-wave tube the attainable efficiency increases with an increase in C, the gain parameter (similar to D defined here), and also in some cases with an increase in the space-charge parameter. Reducing the phase velocity

of the wave toward the end of the tube in order to prevent electrons from slipping into the accelerating phase has been proposed as a means of keeping them in phase with the wave and thus increasing the efficiency. This technique has been tried with some success.

Saturation effects are also observed in crossed-field traveling-wave tubes, but in this case the nature of the effect is quite different. The power output increases with power input up to a point, and thereafter the power output remains at essentially the maximum value. The power output may increase by the amount of increase of the r-f input power or it may decrease slightly if the circuit is lossy. This type of saturation results from the fact that the electrons which have given up all their available potential energy are collected on the circuit. The electrons tend to be focused into the proper phase to give up energy and if the circuit is long enough, eventually they are all collected and the circuit wave is affected only by the losses in the circuit itself. To a first approximation the limiting efficiency in a tube with a lossless circuit does not depend upon the gain parameter or the space-charge parameter in the case of forward-wave interaction, but only on the relative amounts of kinetic energy of the beam and the potential energy available between the position of the beam and the slow-wave circuit.

An estimate of the maximum value of the circuit voltage amplitude can be obtained from a consideration of the beam and circuit geometry. The system used is that shown in Fig. 6, in which a beam containing current I_o is injected at $y = y_o$ into the region between the circuit at $y = d/2$ and the sole at $y = -d/2$. The static electric field is $-E_o \hat{e}_y$, and

the magnetic field is $B_o \hat{e}_x$; the beam is injected at velocity $u_o = E_o/B_o$ and an equivalent potential is defined by $V_o = 1/2 \frac{m}{e} u_o^2$. The total power available from the beam is then

$$P_{available} = I_o V_o + E_o (\frac{d}{2} - y_o) I_o \qquad (V.1)$$

where $I_o V_o$ is the power available in the form of kinetic energy in the beam motion and $E_o(\frac{d}{2} - y_o) I_o$ is the power that could be obtained if the beam traveled through the potential difference between its injection position and that of the circuit. Since

$$\frac{E_o}{V_o} = \frac{2\eta E_o}{\left(\frac{E_o}{B_o}\right)^2} = 2 \frac{\omega_c}{u_o} \qquad (V.2)$$

and

$$\frac{\pi y_o}{d} = r_o, \qquad (V.3)$$

the power available from the beam can be written

$$P_{available} = I_o V_o \left[1 + \frac{\omega_c}{\omega} \beta_e d \, (1 - \frac{2}{\pi} r_o)\right] . \qquad (V.4)$$

The average power carried by the wave on the circuit is

$$P_{ave.} = \frac{1}{2} \frac{|V^2|}{Z_o} = 4A^2 \frac{\omega_c}{\omega} \frac{\sinh^2 \beta_e d}{2} \mp^2 I_o V_o ; \qquad (V.5)$$

in terms of the entrance position of the beam this equation can be written

$$P_{ave.} = 4A^2 I_o V_o \frac{\omega_c}{\omega} \left[\frac{\sinh^2 \frac{\beta_e d}{2} (1 + \frac{2}{\pi} r_o)}{\coth^2 \frac{\beta_e d}{2} (1 + \frac{2}{\pi} r_o)}\right] . \qquad (V.6)$$

If the assumption is made that the average electron velocity does not change, so that $I_o V_o$ is really not available for conversion to wave energy, then the ratio of circuit power to available power can be written

$$\frac{P_{ave.}}{P_{available}} = \frac{4A^2 \sinh^2 \frac{\beta_e d}{2}(1 + \frac{2}{\pi} r_o)}{\beta_e d(1 - \frac{2}{\pi} r_o) \coth \frac{\beta_e d}{2}(1 + \frac{2}{\pi} r_o)} \qquad (V.7)$$

Since the largest possible value for this ratio is one, the maximum value that A can have is

$$A_{max.} = \sqrt{\frac{\beta_e d(1 - \frac{2}{\pi} r_o) \coth \frac{\beta_e d}{2}(1 + \frac{2}{\pi} r_o)}{\sinh \frac{\beta_e d}{2}(1 + \frac{2}{\pi} r_o)}} \qquad (V.8)$$

For the case $\beta_e d = 2.5$ and $r_o = -0.3\pi$, the value of $A_{max.}$ is

$$A_{max.} = 2.82. \qquad (V.9)$$

This value of A is not really the maximum permissible value but only an estimate, since the r-f input power and the kinetic energy in the beam have been disregarded. A circuit amplitude approaching this value would certainly indicate excellent efficiency in terms of the conversion of available potential energy to wave energy.

In order to be able to consider actual numerical values of efficiency, it is necessary to make some assumption about the potential V_o defined by the kinetic energy in the electron beam. Since in magnetron-type tubes the cathode is the sole, V_o is just the d-c potential corresponding to the beam position. In beam type tubes the cathode is usually operated at some potential above the sole potential, and V_o corresponds to a potential less than the d-c potential of the beam position. Throughout the rest of this discussion it will be assumed that the beam originates from an electrode that is at the same potential as the sole and that it is

collected on an electrode at the potential of the circuit. Under this assumption the efficiencies obtained will be slightly lower than those that could possibly be obtained by operating the cathode positive with respect to the sole. If the r-f input power is neglected, the efficiency is

$$\eta = \frac{2A^2 \sinh \frac{\beta_e d}{2} \left(1 + \frac{2}{\pi} r_o\right)}{\beta_e d \coth \frac{\beta_e d}{2} \left(1 + \frac{2}{\pi} r_o\right)} \times 100\ \%, \qquad (V.10)$$

and for the case $\beta_e d = 2.5$ and $r_o = -0.3\pi$,

$$\eta = 10A^2\ \%. \qquad (V.11)$$

Under the assumption that the gain parameter D is small, the efficiency does not depend on D.

5.2 Backward-Wave Oscillator and Amplifier Calculations

The large-signal calculations, including space-charge effects, produced a number of interesting results. Some of these are listed here as a guide to the discussion that follows.

1. At small-signal levels, the phase velocity of the circuit wave is unaffected by the presence of the electron beam even when space-charge effects are included. At large-signal levels, the phase velocity of the circuit wave is only slightly altered by the presence of the beam.

2. The value of the velocity-difference parameter b required for oscillation changes significantly when space-charge effects are included at small-signal levels. The change in b is small at large-signal levels.

3. The starting length of a backward-wave oscillator decreases initially with an increase in the output voltage amplitude when

space-charge effects are small. When these effects are large, the starting length increases at all times for an increase in the output amplitude.

4. The large-signal gain of a backward-wave amplifier decreases with an increase in space-charge effects.

5. A major part of the current is collected on a very short section of the circuit. This limits the average power capabilities of a crossed-field device since a short section of the circuit must dissipate most of the beam power.

6. The electron trajectories at large-signal levels differ appreciably when cases in which space-charge effects have been included are compared with similar cases in which space-charge effects are neglected. The shape of the bunched beam is not significantly changed.

7. A typical value for D is 0.01. For this value of D an appreciable error is introduced at large-signal levels by neglecting the acceleration terms in the equations of motion.

The conditions for backward-wave oscillation were determined as a function of the output voltage amplitude for four values of the space-charge parameter S, i.e., for S = 0, 1.1, 2.2, and 2.9. The procedure for determining the oscillation conditions is to assume a value of A_o and θ_o, the amplitude and phase of the circuit voltage, respectively, at the beginning of the tube (this is actually the output in the case of backward-wave interaction), and a value of b, the velocity difference parameter; the equations are then integrated until the circuit amplitude passes through zero or until it reaches a minimum and begins to increase again, or until it continues to decrease but so slowly that it is impractical to continue the

integration. If the amplitude reaches zero, output occurs for zero input and the tube will oscillate if it is somehow excited into this state.* If the amplitude reaches a minimum and begins to increase again, the velocity parameter was chosen incorrectly for oscillation at the assumed output amplitude and the electron bunches have slipped out of the proper wave phase. If the amplitude continues to decrease slowly, the assumed output amplitude is so large that most of the electrons have been collected on the circuit and very little current remains for interaction with the circuit wave. The last two situations describe a backward-wave amplifier since the application of a signal at the end of the tube having the amplitude given by such a solution and having a frequency corresponding to the value of b would cause the output amplitude A_o. For a given value of A_o, the velocity difference b is varied until the amplitude can be integrated to zero. The length of tube required to maintain oscillation at the amplitude A_o is given by the position at which A reaches zero.

An excellent way to find the value of b required for oscillation is to plot the values of θ as a function of position along the tube. At small-signal levels, θ will be a straight line corresponding to the unperturbed circuit-wave velocity. Fig. 18 is a plot of θ as a function of s for two values of b that caused A to integrate to zero. The calculations refer to a small-signal case for which $S = 2.9$ and the starting length is $s = 1.05$. Values of $b > 3.66$ or $b < 3.62$ did not cause A to integrate to zero, and

---

* In general, the oscillations build up from noise. There are exceptions in which large-signal oscillations would not start spontaneously. These exceptions are discussed later with regard to the starting length of a backward-wave oscillator.

a plot of θ versus s for such cases would deviate from a straight line at an earlier point in s. For $b < 3.62$, θ will eventually increase positively at a faster rate than 3.62 s; for $b > 3.66$, θ will eventually increase negatively at a faster rate than -3.66 s. If space-charge effects are neglected at large-signal levels, θ will still be a straight line (b = 0 always), but when space-charge effects are included, θ will not correspond to the unperturbed circuit velocity ($\theta = -bs$ corresponds to the free-wave velocity). It is still easy to determine the correct value of b because the large rate of change of θ with s still occurs at the end of the tube for incorrect values of b. Fig. 19 is a plot of θ versus s for a large-signal case. Computations for a value of b corresponding to oscillation and for a value of b on either side of the correct value are shown.

A plot of the velocity difference parameter for oscillation as a function of the output amplitude is shown in Fig. 20 for four values of the space-charge parameter S, i.e., S = 0, 1.1, 2.2, and 2.9. As the output amplitude increases, the velocity difference decreases and by the time $A_o = 2.0$, the velocity difference parameter is small and only slightly different for different values of the space-charge parameter. Since the beam spends part of the time near the circuit and part of the time near the sole, the average drift velocity is nearly u_o. Part of the beam is collected on the circuit at large-signal levels and this effectively reduces the space-charge parameter.

The amplitude of the circuit wave as a function of the normalized distance along the tube is plotted in Figs. 21 and 22 for four values of the space-charge parameter S = 0, 1.1, 2.2, and 2.9, with the output

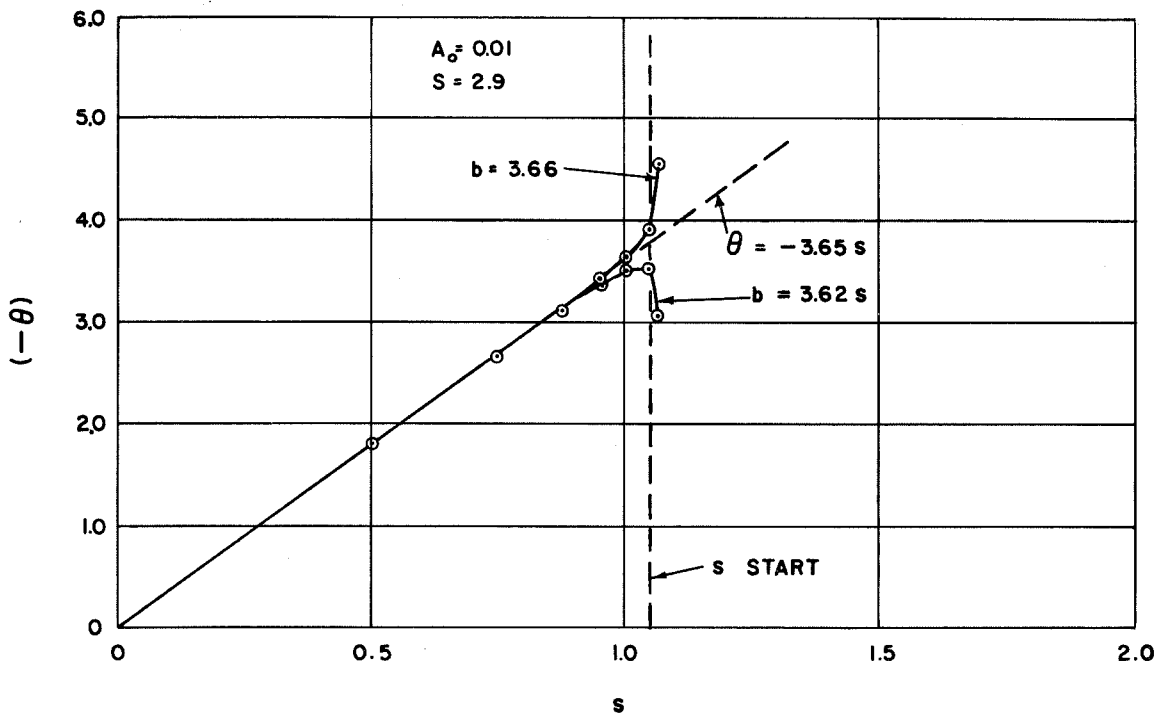

Fig. 18. θ versus s for values of b that correspond to oscillation at small signal levels

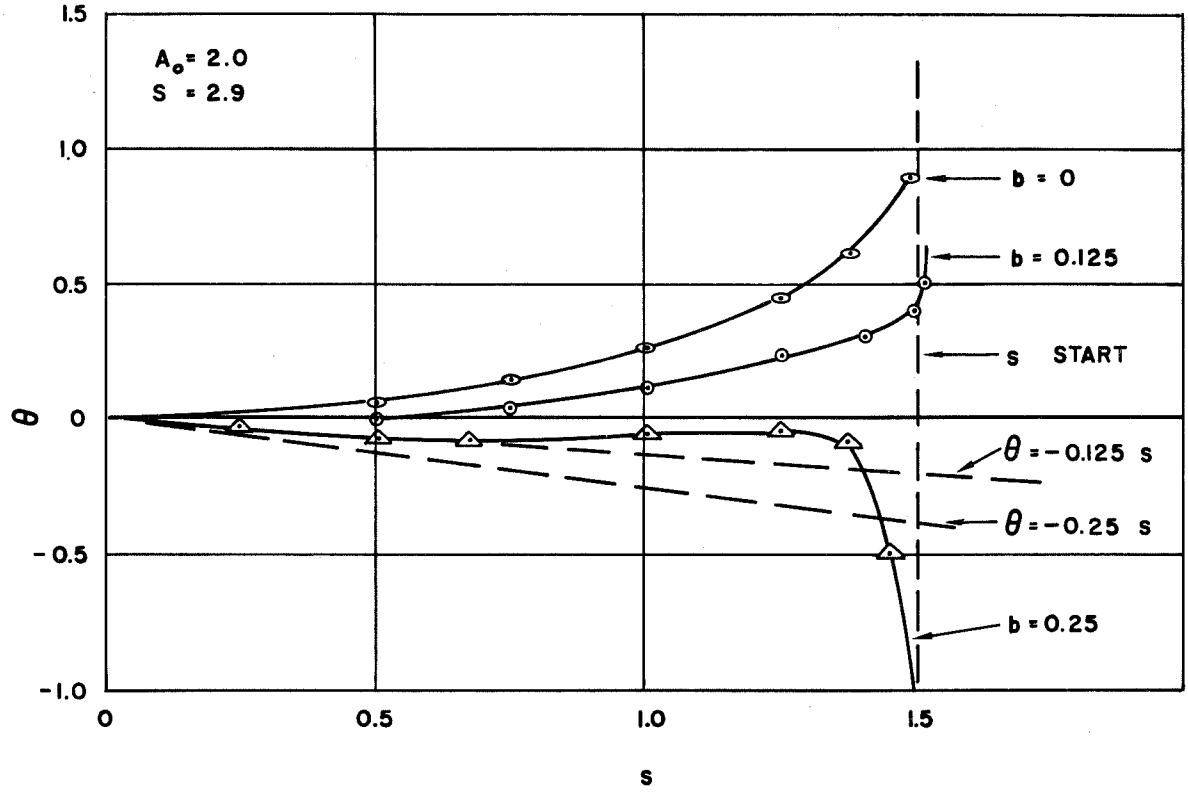

Fig. 19. θ versus s for a large-signal case, b = 0.125 corresponds to oscillation

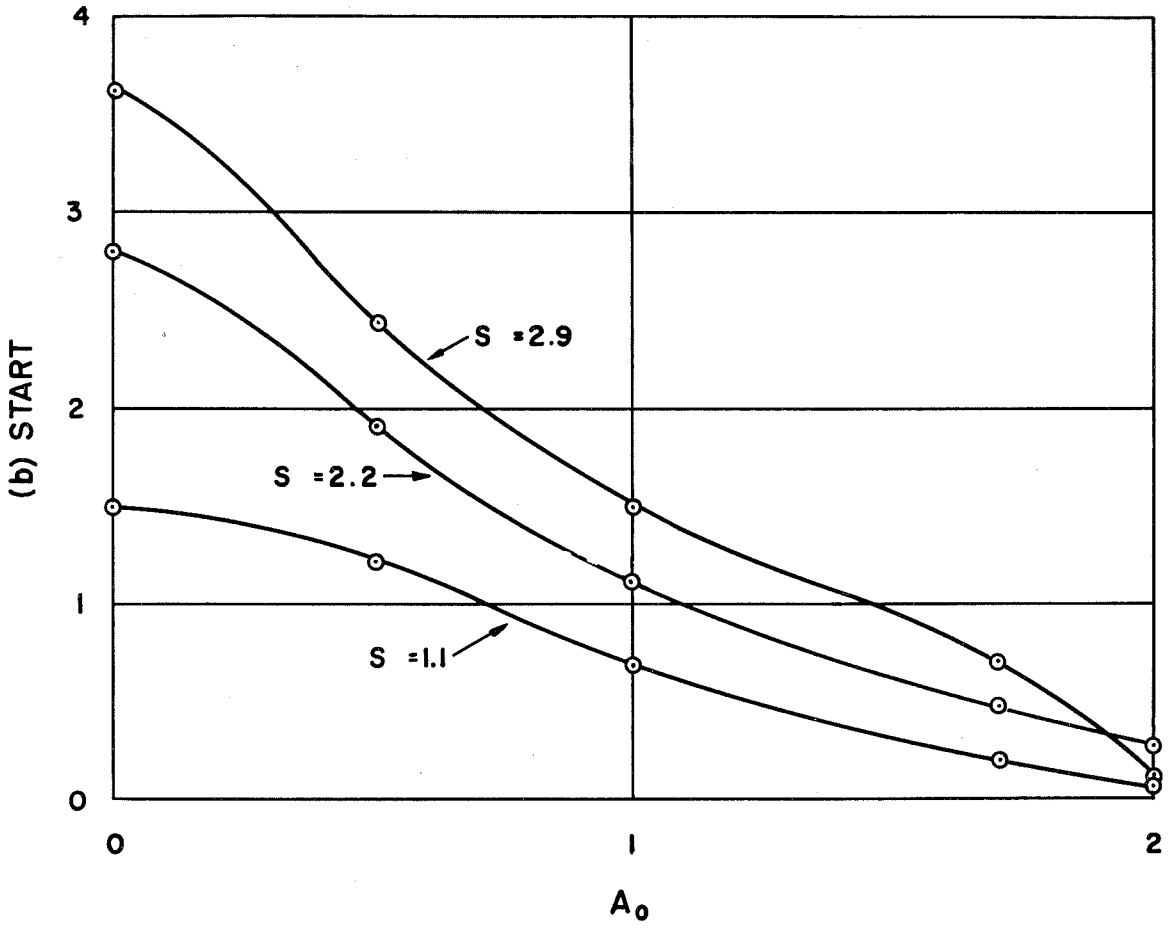

Fig. 20. Velocity parameter for oscillation versus output amplitude wi space charge as the parameter

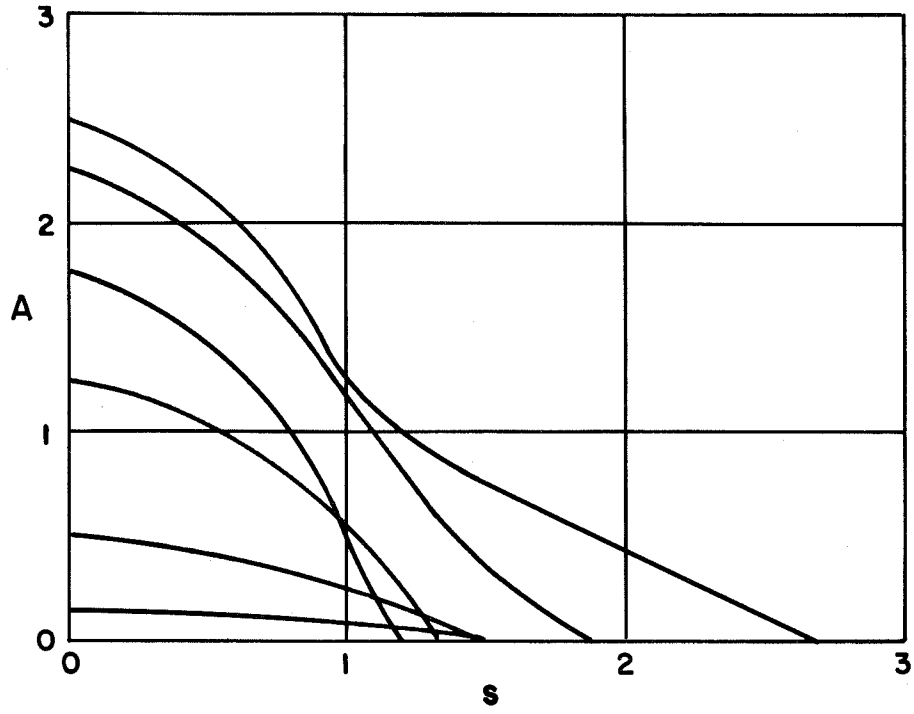

Fig. 21a. Voltage amplitude versus normalized distance, S = 0

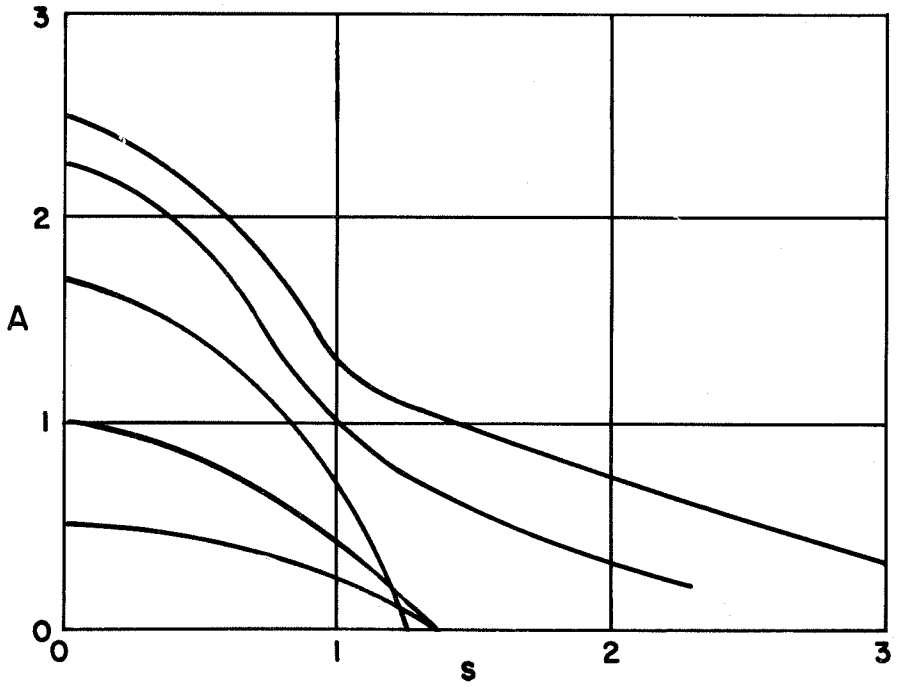

Fig. 21b. Voltage amplitude versus normalized distance, S = 1.1

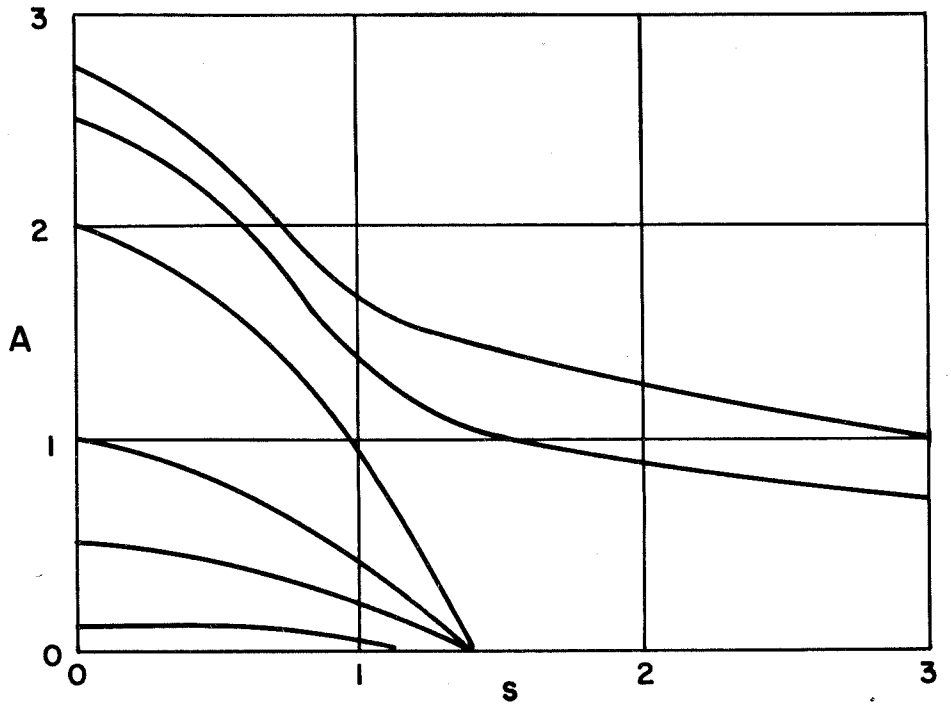

Fig. 22a. Voltage amplitude versus normalized distance, S = 2.2

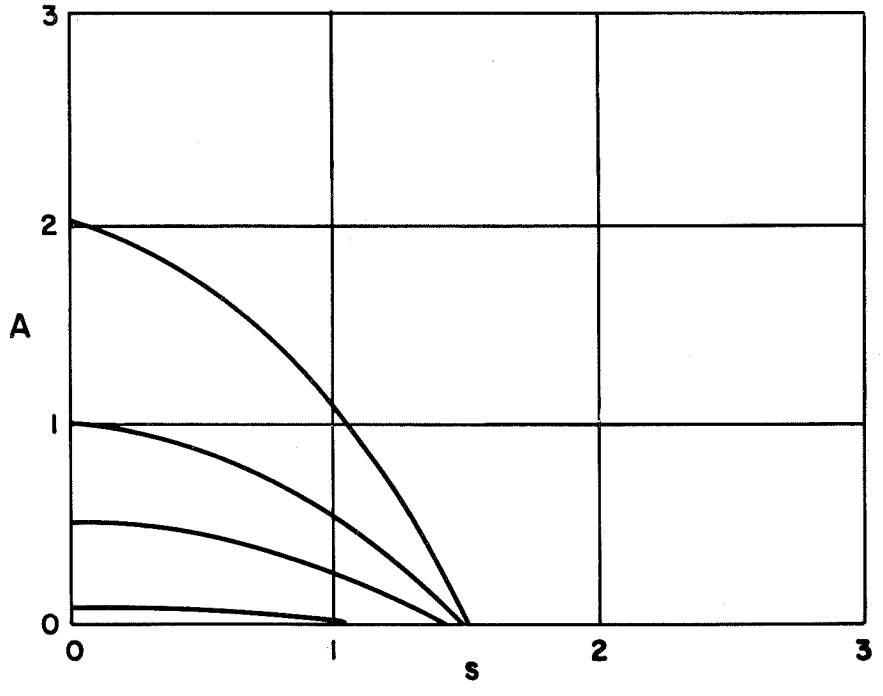

Fig. 22b. Voltage amplitude versus normalized distance, S = 2.9

voltage A_o as the parameter. In Fig. 21a, for S = 0, the tube length required for oscillation decreases as A_o is increased until A_o reaches about 1.75; then the length increases rapidly as A_o is increased. The solutions were carried out only as far as s = 3 because the rate of decrease of A_o with the tube length becomes very small by the time the value s = 3 has been reached. The reason for the initial decrease in starting length* as the amplitude is increased is that as the beam moves closer to the circuit and into regions of stronger fields the effective circuit impedance is increased. Eventually, a part of the beam is collected on the circuit and the starting length increases because the interaction impedance is reduced by the loss of current.

The reduction in starting length with increasing amplitude is also evident for S = 1.1, but it is not so pronounced; for S = 2.2 and S = 2.9 there is no initial reduction in starting length as the amplitude is increased. The increase in starting length with increase in amplitude for the larger values of S can be attributed to the fact that, when space charge is included, the average drift velocity of the beam depends on the location of the beam relative to the circuit and the sole and the phase velocity of the circuit wave changes a little along the length of the tube. This means that a beam which under small-signal conditions was at all times properly phased with respect to the wave, alters its effective drift velocity as

---

* Starting length is really a misnomer when applied to these cases; although a tube of this length would oscillate if it were excited, the oscillation would not build up from noise because the small-signal starting length is actually greater than the tube length.

it proceeds down the tube under large-signal conditions and that the velocity cannot be ideal for interaction at all times but must be reasonably good over the entire length of the tube. The cases in Figs. 21 and 22 in which A_o is so large that the amplitude has not reached zero were computed with b = 0. Values of b in the neighborhood of zero were tried but the wave amplitude did not decrease any more rapidly. Several values of b appreciably different from zero were also used, and the gain decreased rapidly as b was varied about the optimum value. For example, a case with $A_o = 2.0$, S = 2.2, and b = 3 was integrated to a minimum of A = 1.1 and then began increasing again.

A comparison of the circuit amplitude at s = 2 for the different space-charge cases with $A_o = 2.5$ in Figs. 21 and 22 shows that the gain decreases as the space-charge parameter is increased. For S = 0 the voltage gain is 2.5/0.45 = 5.6, for S = 1.1 it is 2.5/0.74 = 3.4, and for S = 2.2 it has dropped to 2.5/0.9 = 2.8. For S = 2.2 the rate of decrease of A with s is so small toward the end of the tube that it would not be practical to try to increase the voltage gain beyond about three by increasing the tube length. This decrease in gain with an increase in space-charge effects can be attributed to the fact that because the circuit velocity is chosen for the best over-all interaction, the electrons that have not been collected in the first part of the tube will not necessarily be in the proper phase or travel with the proper velocity for optimum interaction near the end of the tube.* In addition, when space-charge

* This effect is more important in the backward-wave cases than in the forward-wave cases because of the "narrow-band" nature of backward-wave interaction; i.e., if the electron bunch travels more slowly than the wave, it tends to increase the wave-velocity and to increase the velocity difference. In forward-wave interaction, the electron bunch tends to pull the wave along with it and to maintain synchronism.

effects are included, those electrons that are in such a phase as to receive energy from the wave initially, are forced closer to the sole by the space-charge forces and therefore are in regions of weaker circuit fields than when space-charge forces are neglected.

In Fig. 23 the percentage of the electrons that have been collected on the circuit is plotted as a function of distance along the circuit for $A_o = 2.5$ and $S = 0$ and 2.2. There is little difference in the rate at which electrons are collected on the circuit for $S = 0$ and $S = 2.2$. There are two interesting effects to be noted in this curve. The first is that about 50 percent of the electrons are collected on a very short section of the circuit. This severely restricts the average power that a backward-wave, crossed-field device can deliver since the circuit itself must be capable of dissipating the beam power. Since s is proportional to the interaction parameter, a smaller value of D would imply that the beam was being collected on a longer physical length of circuit and therefore such a device would be able to operate at a higher average power level. The second point of interest in Fig. 23 is that the number of electrons collected is leveling off at about 70 percent. Equations V.9 and V.11 indicate that 100 percent conversion of available beam energy would correspond to 80 percent over-all efficiency. Seventy percent electronic efficiency would therefore imply an over-all efficiency of about 55 percent and this value is probably close to the practical limit of efficiency for a beam-type backward-wave amplifier. The reason for this limit is that in a backward-wave device, the circuit fields are weak near the end of the tube and the part of the beam that remains has

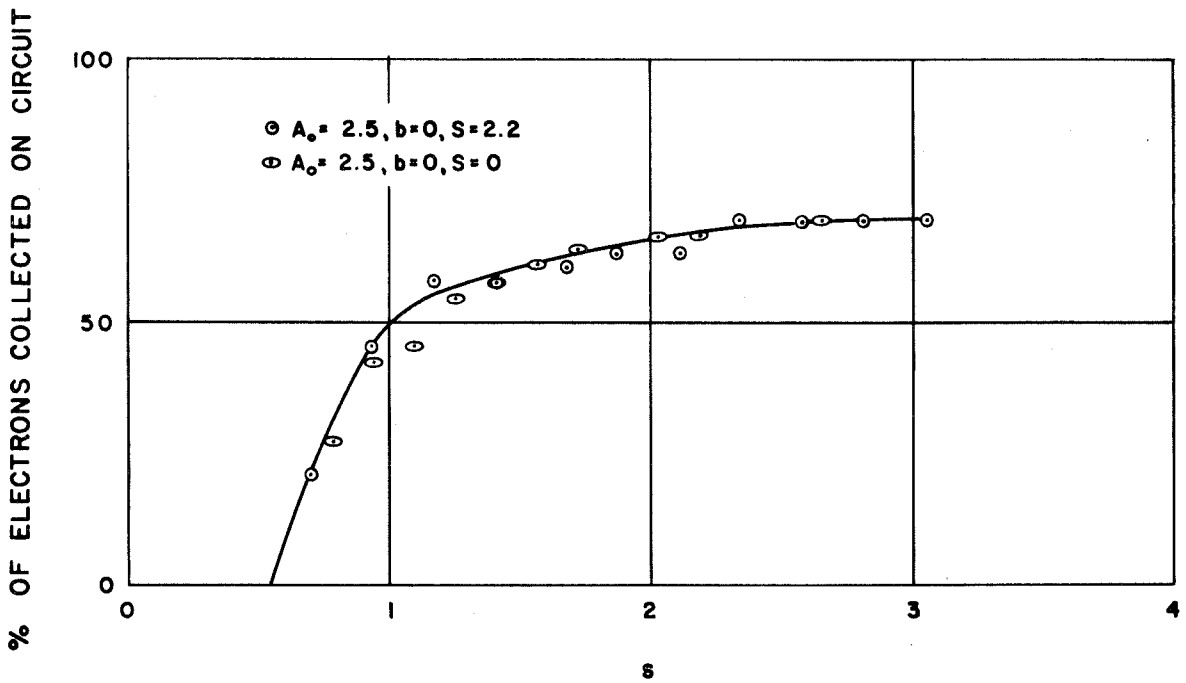

Fig. 23. The percentage of the electrons collected on the circuit as a function of position for large-signal backward-wave interaction

been moved down toward the sole. It is not practical to build the tube long enough to make use of this remaining current which is in a very unfavorable position for interaction.

An electron-phase plot for a large-signal case with $A_o = 1.75$ and $S = 0$ is shown in Fig. 24 and a similar plot with $A_o = 2.0$ and $S = 2.2$ is given in Fig. 25. The solid lines represent the electron trajectories in transverse position and phase, and the dashed lines correspond very closely to the beam shape at several different values of s. The trajectory curves are plotted for only half of the electrons actually used in the computations. Fig. 24 shows the formation of the so-called "spoke" of electrons (in magnetron terminology) in a symmetric pattern about $\phi = \pi/2$. It is clear from this figure why the circuit phase is unchanged in the absence of space charge. The field terminating on the circuit is symmetric about $\phi = \pi/2$; therefore, the fundamental component is purely a sine term and since the circuit phase velocity is proportional to the cosine term alone under small-D assumptions, it does not change. From an equivalent circuit point of view, the bunches of charge form at a maximum of the longitudinal electric field or at a zero of the voltage. The displacement current flowing into the circuit is the time rate of change of the field terminating on the circuit and this rate of change is zero at the center of the bunch. The displacement current is π out of phase with the voltage, and the electron beam appears as a pure negative resistance to ground. If this equivalent resistance is large compared with the impedance of the shunt elements in the equivalent circuit, the phase velocity will not be affected appreciably. This

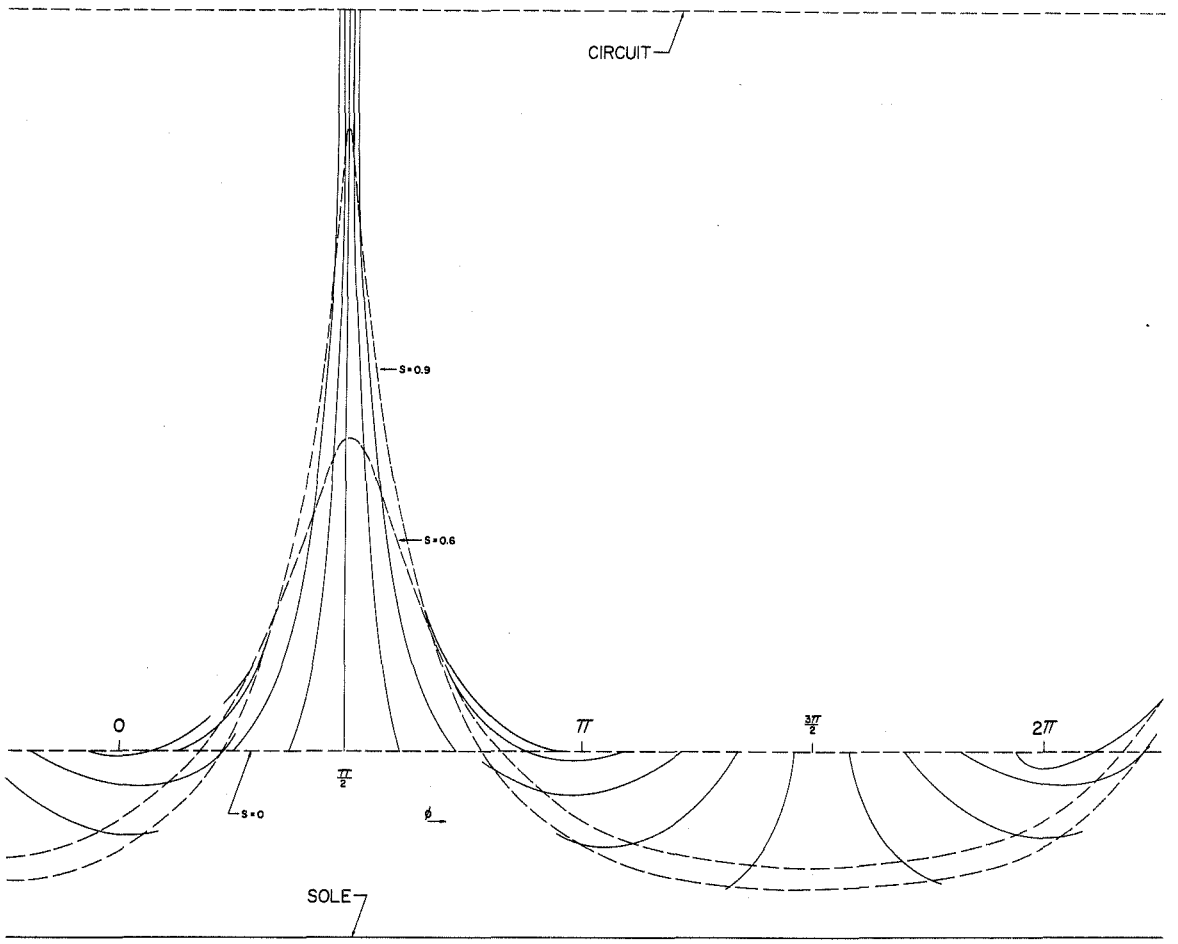

Fig. 24. Large-signal electron phase trajectory plot, $A_o = 1.75$, $S = 0$

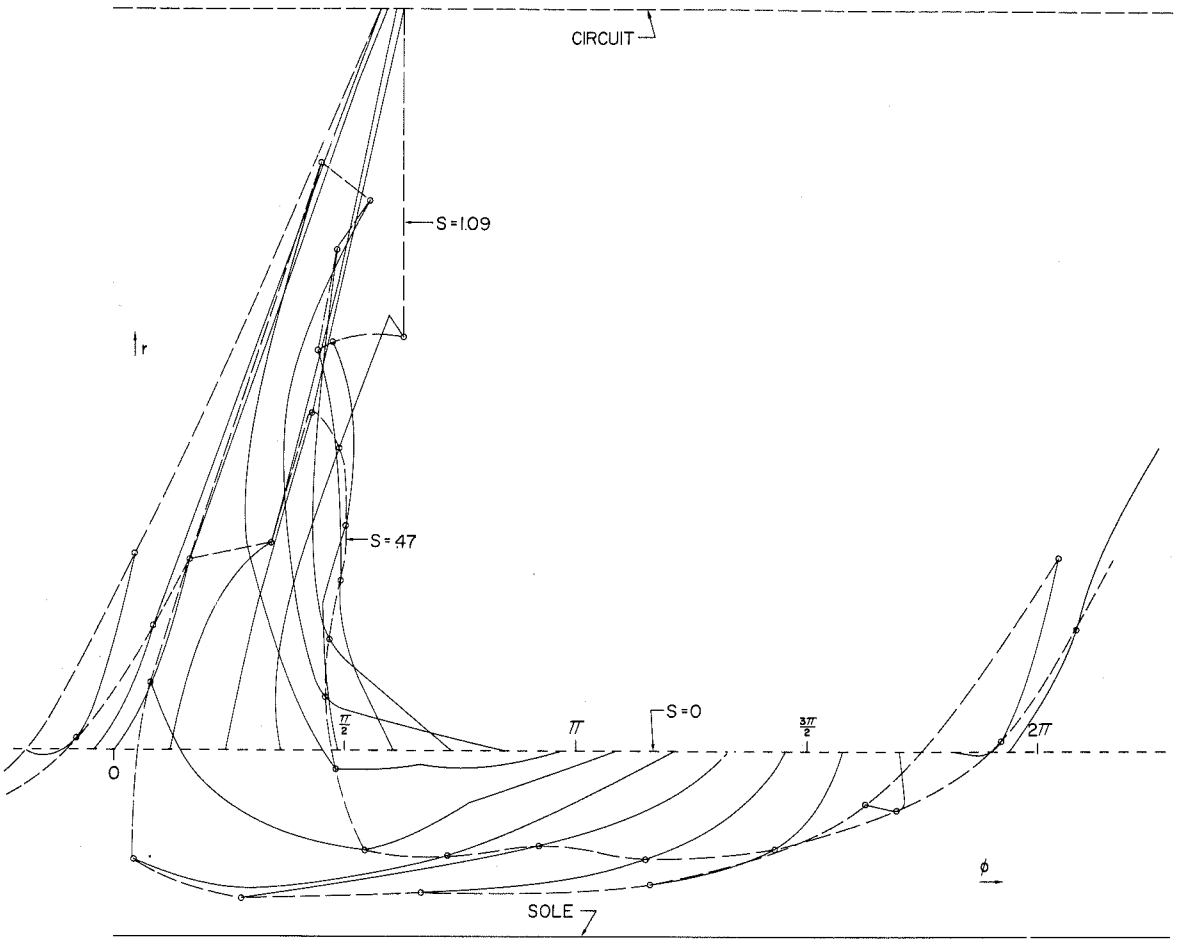

Fig. 25. Large-signal electron phase trajectory plot, $A_o = 2.0$, $S = 2.2$

condition is met by the small-D approximations. An electron "spoke" is also apparent in the phase trajectory plot for $A_o = 2.0$, $S = 2.2$ (Fig. 25), but the spoke is not symmetric about $\phi = \pi/2$. If the spoke were to form as it does when space charge is neglected, then the space-charge forces would tend to force the top of the spoke ahead in phase, and the charge between $\phi = -\frac{\pi}{2}$ and $\frac{\pi}{2}$ would be pushed toward the circuit, while that between $\phi = \pi/2$ and $3\pi/2$ would be forced away from the circuit. As a result the effective bunch would be located at $\phi < \pi/2$ and the circuit wave would be speeded up. The general shape of the spoke is quite similar for the two cases shown in Figs. 24 and 25.

An examination of the magnitude of some of the terms neglected in the equations of motion reveals that in the large-signal calculations, terms as large as 20D were neglected with respect to one. This could mean that there would be considerable error in applying these results to a tube for which the value of D is 0.01. Since the large errors occur for electrons that are close to the circuit and are about to be collected, it is possible that the over-all effect is not great. These errors could be eliminated by specifying a value of D and including all the terms in the equations of motion.

Another possible source of error in the large-signal computations should be pointed out. In order to compute the driving term in the circuit equation, a Fourier analysis in time (or phase) of the fields terminating on the circuit at the particular z position corresponding to m must be carried out. One way to do this would be to specify a phase at z, locate the positions of all the electrons when the phase at z is as

specified, and compute the flux terminating on the circuit at z due to all the electrons. Now allow the phase to advance by a fixed increment and repeat the procedure. Continue to repeat this procedure for a period of 2π in phase and then apply a Fourier analysis to the results. To save computing time, instead of specifying the phases independently, they were specified by the time of arrival of the individual electrons at the particular z position. In this way, in the process of computing the space-charge force on an electron when it is at z, all the functions necessary to compute the flux terminating on the circuit are also obtained. The disadvantage of this method, however, is that the increments in phase are not equal. There is also some difficulty when electrons are collected on the circuit. In order to use the same integration routine, it is convenient to have the same number of points in phase at all times. The procedure that was used was to include a fictitious electron (a point in phase) whenever an electron was collected on the circuit. The phase of this fictitious electron was chosen as the average phase of the nearest two electrons. Unfortunately, all the electrons are collected at almost the same phase so that, although the number of increments in phase remained constant, most of the increments were very small and the effective number was just the number of uncollected electrons. This is a difficulty that could be eliminated by choosing the phase of the fictitious electron to be in a region where there are few electrons.

5.3 Forward-Wave Amplifier Calculations

A limited number of large-signal calculations were carried out under forward-wave interaction conditions with $S = 0$ and $S = 2.2$. The

procedure in this case is to assume a value of A_o, θ_o, and b and then integrate the equations until the voltage amplitude no longer increases with s. Calculations were carried out only for $A_o = 0.2$, 0.5, and 0.75 because, for smaller A_o, the tube must be unreasonably long for saturated output (small-signal analytical work could be used to determine the behavior for small A), and for larger A_o the possible voltage gain is small. The results are subject to the same errors discussed at the end of the preceding section. The errors introduced by the collection of electrons on the circuit are even more significant in this case because virtually all the electrons are collected on the circuit. Some of the interesting results obtained are:

1. The circuit phase velocity is only slightly affected by including space-charge forces.

2. The large-signal gain appears to be slightly decreased by the presence of space-charge, although the effect may be within the limit of computational errors (the small-signal gain is increased by space-charge effects[6]).

3. The obtainable efficiency does not seem to be affected by space charge.

4. A large fraction of the beam current is collected on a relatively short section of the circuit.

A graph of the phase difference θ as a function of position along the tube is shown for $A_o = 0.75$ and $S = 2.2$ in Fig. 26. The curves are plotted for three values of the velocity difference parameter $b = -0.125$, 0, and 0.25. Although the value $b = 0$ gave maximum gain, the gain was only

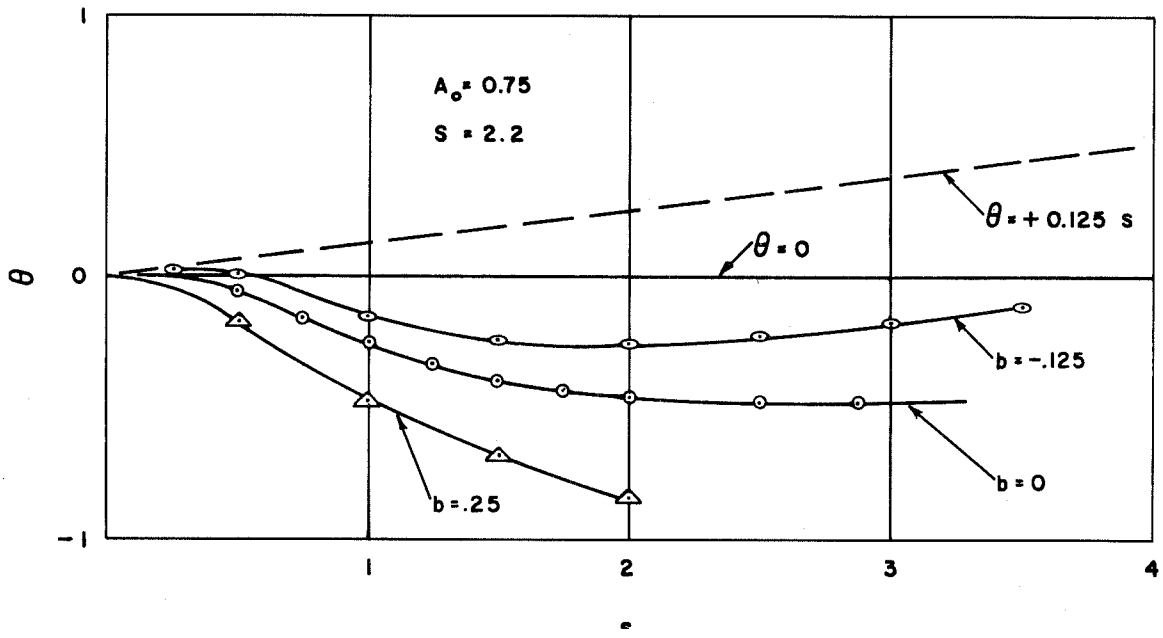

Fig. 26. θ versus s for large-signal forward-wave amplifier computations

slightly higher than in the other two cases. The change in wave velocity is small, just as it was in the case of backward-wave interaction.

In Fig. 27 the voltage amplitude as a function of position along the tube is plotted for S = 0 and S = 2.2. The space-charge computations are for the value of b that gave the maximum gain for a given value of A_o. A comparison of the amplitudes at s = 2 for the cases in which $A_o = 0.75$ would imply that the large-signal gain when space charge effects are included is somewhat less than if space charge is neglected. For S = 2.2, the gain is 2.42/0.75 = 3.23, and for S = 0, the gain is 2.55/0.75 = 3.4. The limiting value of A appears to be about the same for both cases; it is about 2.9 for $A_o = 0.75$. The efficiency in this case is

$$10(A_m^2 - A_o^2) = 10\left[(2.9)^2 - (0.75)^2\right] = 79\%.$$

Since "maximum" efficiency is 80 percent for the geometry used in these computations, the efficiency of conversion of potential energy to wave energy is almost 100 percent. The same situation is true for the cases with smaller values of A_o. The reason for this excellent efficiency in the case of forward-wave interaction is that the wave amplitude is large at the end of the tube and even the electrons close to the sole can be captured and used.

The percentage of the electrons collected on the circuit is shown as a function of position for several forward-wave-interaction cases in Fig. 28. A large percentage of the electrons are collected on a short length of tube just as in backward-wave interaction, but thereafter

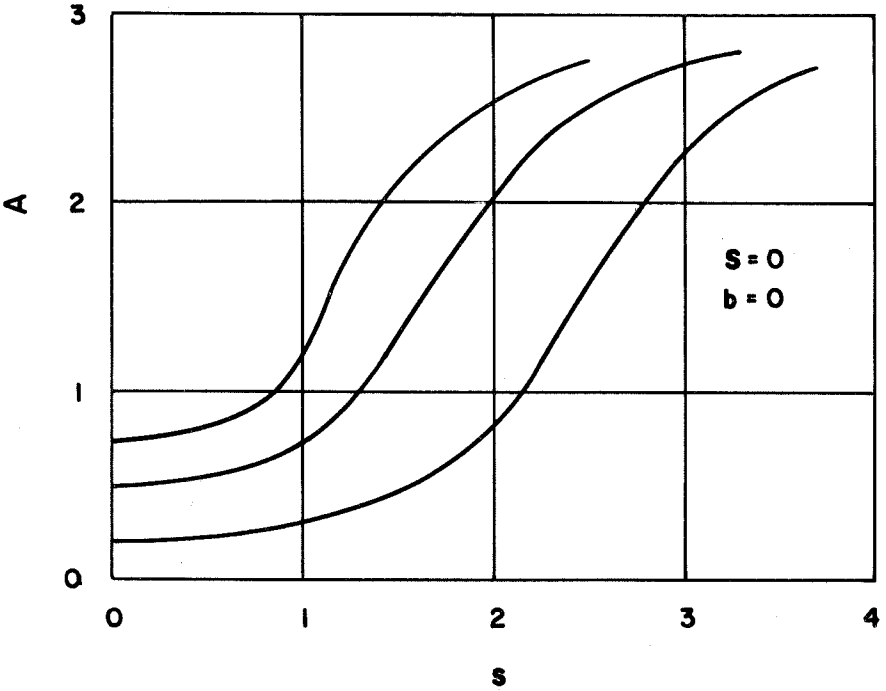

Fig. 27a. Amplitude versus normalized distance for forward-wave interaction, S = 0

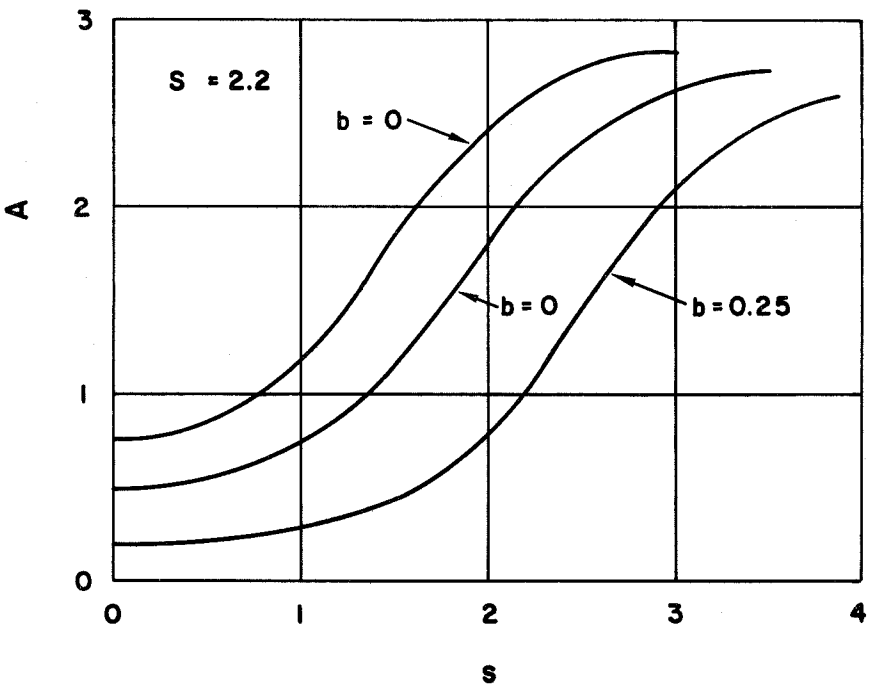

Fig. 27b. Amplitude versus normalized distance for forward-wave interaction, S = 2.2

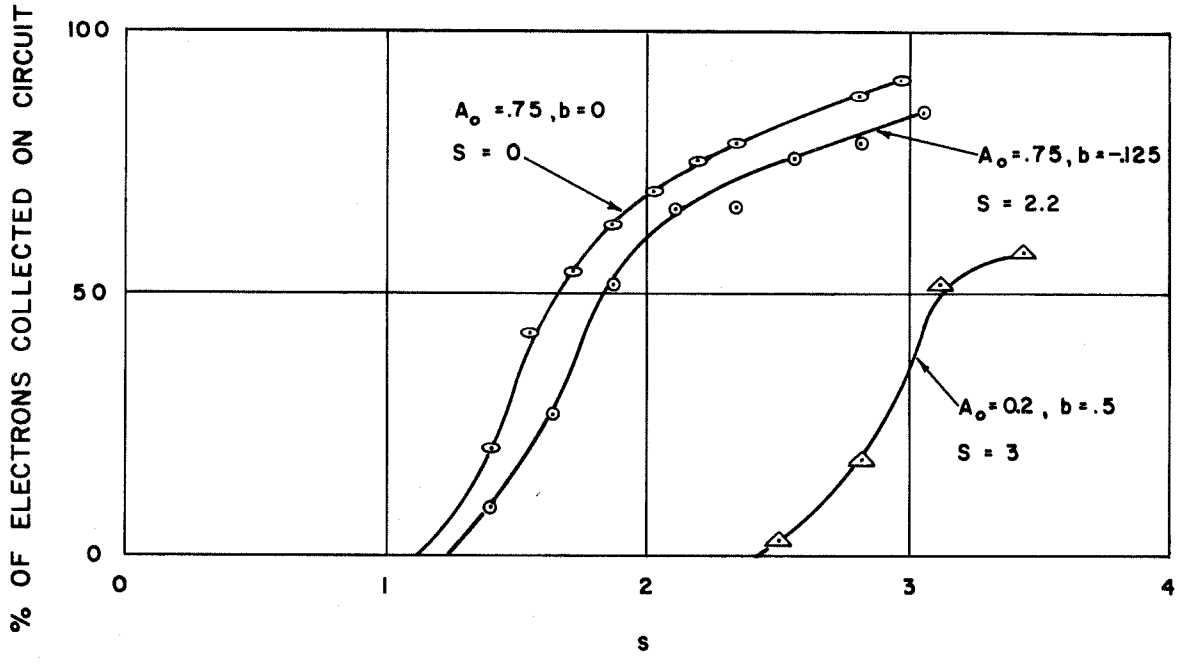

Fig. 28. The percentage of the electrons collected on the circuit as a function of position for large-signal forward-wave interaction

electrons continue to be collected until virtually all the charge is gone from the beam. The efficiency does not appear to depend on the space-charge parameter S for forward-wave interaction.

VI. CONCLUSION

The integro-differential equations describing beam-type, crossed-field, traveling-wave tubes presented in Chapter II and the large-signal calculations presented in Chapter V constitute the major results of this investigation. In this section, some of the significant effects that are indicated by the computations will be pointed out and a few comments will be made regarding this technique for solving the problem.

1. The effects of space charge are more important in backward-wave interaction than in forward-wave interaction. In backward-wave interaction, the disorder in the beam that results from the nonlinear effects increases as the amplitude of the circuit wave decreases and the wave is unable to interact as favorably with the beam. The "narrow-band" nature of backward-wave interaction contributes to this decrease in favorable interaction.

2. The large-signal starting length of a backward-wave oscillator is increased and the gain of a backward-wave amplifier is decreased. Practically speaking, this implies that the efficiency of a backward-wave oscillator is also decreased because, for a given length of tube, the oscillation will occur at a lower level. The computations for a relatively large value of the space-charge parameter indicate that a gain of about 10 db and an efficiency of 60 percent constitute good performance characteristics for a large-signal, backward-wave amplifier.

3. There appears to be very little difference in the results for forward-wave interaction regardless of whether space-charge forces are included or neglected; however, the large-signal gain is possibly reduced a little.

4. The efficiency does not depend on the gain parameter D; i.e., for the same normalized length of tube, the efficiency is the same. This result follows from writing the system equations in normalized variables. Under the assumption that $D \ll 1$, the average power carried by the circuit wave (equation V.5) does not depend on D. This conclusion must be tempered by a practical consideration, however, since loss on the circuit and beam defocusing reduce the efficiency as D is made smaller. (The tube length is normalized, $s = \beta_e Dz$, so that a smaller value of D means that the tube must be physically longer.)

5. A large fraction of the beam is collected on a short length of circuit. A smaller value of D means that the beam is collected on a greater physical length of circuit and this would increase the average power capabilities of the tube.

The solution of the equations presented in Chapter II can be carried out only on a large-scale digital computer. The computation of the space-charge forces by summing the forces due to the individual equivalent electrons is extremely time-consuming. With IBM 704 equipment a single integration step in s requires 20 seconds for a thin-beam case with N = 33. Since the integration interval used was $s = 1/64$, it requires 20 minutes to integrate from s = 0 to s = 1. A brief study of the numerical errors indicates that it would be desirable to use $\Delta s < 1/64$ and $N > 33$ for some of the space-charge cases. Since the computing time is inversely proportional to Δs and approximately proportional to N^2, it is impractical to attempt to achieve great accuracy in the numerical solutions.

Replacing the thin electron beam by a set of equivalent line charges resulted in a buildup of computer errors that masked the beam-wave interaction effects. This buildup is similar to that observed physically in thin hollow, cylindrical beams of electrons. The buildup of computer errors was eliminated by assuming that the short-range force between line charges was zero, and an equivalent space-charge parameter was defined to bring the results into agreement with small-signal theory. The buildup of computer errors might also have been eliminated by using an electron beam of finite thickness. Simulation of a thick beam, which might require five layers of N electrons, would be completely impractical in terms of computing time. A new and clever means of calculating the space-charge forces would be the only possible way such a problem could be solved in a reasonable time on presently available computing machines.

An interesting calculation that might be carried out using the thin-beam equations would be to allow for cycloidal trajectories in the unperturbed electron beam. Since a calculation of this type would require specifying a value for D, it would also be possible to include the acceleration terms in the equations of motion with no additional loss of generality. An examination of the magnitudes of some of the terms neglected under the small-D assumption indicated that these terms were not always negligible when a value of D = 0.01 was assumed.

It would appear that for the values of the space-charge parameter considered in this study, forward-wave calculations could be carried out

without any consideration of space-charge forces. It would then be possible to allow for a finite thickness of the electron beam.

APPENDIX

THE FIELDS OF A SLOW WAVE ON A TWO-DIMENSIONAL CIRCUIT

Consider a system which has a slow-wave circuit at $y = d/2$ which will propagate a wave in the z direction, and a flat conducting plate at $y = -d/2$. The actual circuit structure is of no consequence since we are interested only in the variation of the fields with distance across the interaction space, provided that the circuit will support a slow wave. We will consider only transverse magnetic waves so that all field components can be derived from the z component of electric field. In the absence of any charge in the region between the circuit and the sole, E_z must satisfy

$$\nabla^2 E_z - \mu_o \epsilon_o \frac{\partial^2 E_z}{\partial t^2} = 0 \qquad \text{(A.1)}$$

If time and z dependence $e^{j(\omega t - \beta z)}$ are assumed, and there are no variations with x, equation A.1 can be written

$$\frac{\partial^2 E_z}{\partial y^2} + (\omega \mu_o \epsilon_o - \beta^2) E_z = 0; \qquad \text{(A.2)}$$

if the phase velocity of the wave is much less than the velocity of light $\omega^2 \mu_o \epsilon_o$ can be neglected with respect to β^2 and the solutions to equation A.2 are just

$$E_z = (A \sinh \beta y + B \cosh \beta y)\, e^{j(\omega t - \beta z)} \qquad \text{(A.3)}$$

where A and B are arbitrary constants to be determined by the boundary conditions. The boundary condition at the sole is that the tangential electric field be zero, so that

$$E_z = A \sinh \beta \left(y + \frac{d}{2}\right) e^{j(\omega t - \beta z)} \quad . \tag{A.4}$$

The remaining fields can be derived from equation A.4. The only nonzero fields are

$$H_x \cong - \frac{j\omega \epsilon_o}{\beta^2} \frac{\partial E_z}{\partial y} = - \frac{j\omega \epsilon_o}{\beta} A \cosh \beta \left(y + \frac{d}{2}\right) e^{j(\omega t - \beta z)} \tag{A.5}$$

and

$$E_y \cong \frac{j}{\beta} \frac{\partial E_z}{\partial y} = j A \cosh \beta \left(y + \frac{d}{2}\right) e^{j(\omega t - \beta z)} \tag{A.6}$$

The fact that the expression $\omega^2 \mu_o \epsilon_o$ can be neglected with respect to β^2 means that E_z satisfies Laplace's equation; hence the electric fields could equally well be derived from a potential function.

LIST OF SYMBOLS

$A(z)$	Normalized amplitude of the circuit wave
B_o	Static magnetic field in the x direction
b	Velocity difference parameter; $u_o = v_o(1 + Db)$
C	Capacitance per unit length of the equivalent transmission line
D	Crossed-field tube gain parameter; (equation II.32)
d	Distance between the circuit and the ground plate (sole)
E_o	Static electric field between the circuit and the sole in the absence of space charge
E_y, E_z	Total electric field
E_{sy}, E_{sz}	Electric field due to space charge
e	Magnitude of electronic charge
$\hat{e}_x, \hat{e}_y, \hat{e}_z$	Unit vectors in the directions of the coordinate axes
F	Function relating the flux terminating on the circuit at z to the charge at y', z'; (equation II.17)
g	Space-charge parameter for thick beams; (equation II.50)
h	Integration interval in s; $\Delta s = h$
I_o	Total current in the unperturbed beam
$i(z,t)$	Current per unit length flowing into the equivalent transmission line
$i_1(z,t)$	Fundamental component (in time) of current per unit length flowing into the transmission line
$i_1(y_o)$	Current density in the unmodulated beam
i_2	Average current density in the unmodulated beam

K	Combination of constants; (equation II.31)
L	Inductance per unit length of the equivalent transmission line
m	Integer giving z (or s) position in difference equations (also used for electronic mass in Chapter II)
N	Number of equivalent line charges ("electrons") in a phase period of 2π
p, q	Normalized y and z velocities of the electrons
q_ℓ	Charge per unit length of a line charge
r, s	Normalized y and z coordinates; $r = \pi y/d$, $s = D\beta_e z$
s_m^{ij}	Difference between s positions of electrons i and j when i is at m
S	Space-charge parameter for thin beams;(equation II.85)
t_m^{ij}	Difference in r positions of electrons i and j when i is at m
t	Time, seconds
u_o	Average electron drift velocity in the z direction in the absence of space charge; $u_o = E_o/B_o$
$u_1(y)$	Velocity of the electrons in the z direction as they enter the interaction region
$V(z,t)$	Voltage on the equivalent transmission line
$V(y,z,t)$	Potential function describing the fields of a single spatial harmonic of a wave on the slow-wave circuit
V_o	Voltage corresponding to kinetic energy of the beam; $\frac{1}{2} mu_o^2 = eV_o$
v_o	Phase velocity of a free wave on the transmission line; $v_o = \frac{1}{\sqrt{LC}}$

w	Width of the circuit in the x direction
x,y,z	Rectangular coordinates; z is along the direction of beam flow and y is across the interaction space
y_o, z_o	Coordinates of charge in the beam at time t = 0
Y	Function relating the electric field in the y direction at y, z to the charge at y', z';(equation II.20)
Z	Function relating the electric field in the z direction at y, z to the charge at y', z';(equation II.21)
Z_o	Impedance parameter at the plane of the circuit;(equation II.3)
α	Magnitude of the ratio of the r-f electric field of the circuit in the y direction to that in the z direction at the beam entrance position
β	Propagation constant of a wave $\beta = \frac{\omega}{v_{phase}}$
β_e	Propagation constant of electrons, $\beta_e = \omega/u_o$
ϵ	Dielectric constant of vacuum
η	Magnitude of electronic charge to mass ratio (also used for efficiency in Chapter V)
$\theta(z)$	Negative of the difference between the actual wave phase and the phase of a wave traveling with velocity u_o
ρ	Charge density
ρ_1	Average charge density in unmodulated beam
τ	Beam thickness in y direction
$\phi(z,t)$	Phase of the circuit wave
0^2	Factor which relates impedance at the circuit to impedance at the beam; $Z(y_o) = Z_o \mathbb{0}^2$

ω Radian frequency of r-f signal

ω_c Cyclotron frequency; $\omega_c = \eta\beta_o$

ω_p^2 Plasma frequency defined by the average charge density ρ_1

REFERENCES

1. Warnecke, R. R., Guenard, P., Doehler, O., and Epstein, B., "The M-Type Carcinotron Tube," Proc. IRE (1955), 43, 413-424

2. Pierce, J. R., Traveling-Wave Tubes, D. Van Nostrand, New York, (1950).

3. Muller, M., "Traveling-Wave Amplifiers and Backward-Wave Oscillators," Proc. IRE, (1954), 42, 1651-1658.

4. Feinstein, J., and Kino, G., "The Large-Signal Behavior of Crossed-Field Traveling-Wave Devices," Proc. IRE (1957), 45, 1364-1373.

5. Gould, R. W., "A Field Analysis of the M-Type Backward-Wave Oscillator" Technical Report No. 3, Electron Tube and Microwave Laboratory, California Institute of Technology (1955).

6. Gould, R. W., "Space-Charge Effects in Beam-Type Magnetrons," J. App. Phys. (1957), 28, 599-605.

7. Nordsieck, A. T., "Theory of the Large-Signal Behavior of Traveling-Wave Amplifiers," Proc. IRE (1953), 41, 630-637.

8. Poulter, H. C., "Large-Signal Theory of the Traveling-Wave Tube," Technical Report No. 73, Electronics Research Laboratory, Stanford University (1954).

9. Tien, P. K., Walker, L. R., and Wolontis, V. M., "A Large-Signal Theory of Traveling-Wave Amplifiers," Proc. IRE (1955), 43, 260-277.

10. Rowe, J. E., "A Large-Signal Analysis of the Traveling-Wave Amplifier," Technical Report No. 19, Electron Tube Laboratory, University of Michigan (1955).

11. Gould, R. W., "Interaction of an Electron Beam with a Periodic Circuit," Technical Report No. 1, Electron Tube and Microwave Laboratory, California Institute of Technology (1955).

12. Smythe, W. R., Static and Dynamic Electricity, McGraw-Hill Book Company (1950), 85-86.

13. Heffner, H., "Analysis of the Backward-Wave Traveling-Wave Tube," Proc. IRE (1954), 42, 930-937.

14. Johnson, H. R., "Backward-Wave Oscillators," Proc. IRE (1955), 43, 684-697.

15. Kyhl, R. L., Webster, H. E., "Breakup of Hollow Cylindrical Electron Beams," IRE Trans. Elect. Devices (1956), 4, 172-183.

16. Gould, R. W., "Theory of Hollow Beam Instabilities," Paper presented at the Electron Tube Research Conference, Boulder Colorado (1956).

17. Pierce, J. R., "Instability of Hollow Beams," IRE Trans. Elect. Devices (1956), 4, 183-189.

18. Kompfner, R., Results of some numerical computations on sheet electron beams presented informally at Cornell University Conference on Electron Beam Production and Focusing (1956).